

## Large-scale differences in functional organization of left- and right-handed individuals using whole-brain, data-driven analysis of connectivity

Link Tejavibulya<sup>1</sup>, Hannah Peterson<sup>2</sup>, Abigail Greene<sup>1,3</sup>, Siyuan Gao<sup>4</sup>, Max Rolison<sup>5</sup>, Stephanie Noble<sup>2</sup>, Dustin Scheinost<sup>1,2,4,5,6</sup>

1. Interdepartmental Neuroscience Program, Yale School of Medicine, New Haven CT
2. Department of Radiology and Biomedical Imaging, Yale School of Medicine, New Haven CT
3. MD/PhD Program, Yale School of Medicine, New Haven CT
4. Department of Biomedical Engineering, Yale University, New Haven CT
5. Child Study Center, Yale School of Medicine, New Haven CT
6. Department of Statistics and Data Science, Yale University, New Haven CT

## 1 **Abstract**

2 Handedness influences differences in lateralization of language areas as well as dominance of  
3 motor and somatosensory cortices. However, differences in whole brain functional organization  
4 due to handedness have been relatively understudied beyond pre-specified networks of interest.  
5 Functional connectivity offers the ability to unravel differences in the functional organization of  
6 the whole brain. Here, we compared connectivity profiles of left- and right-handed individuals  
7 using data-driven parcellations of the whole brain. We explored differences in connectivity  
8 profiles of previously established regions of interest, and showed functional organization  
9 differences between primarily left- and primarily right-handed individuals in the motor,  
10 somatosensory, and language areas using functional connectivity. We then proceeded to  
11 investigate these differences in the whole brain and found that the functional organization of left-  
12 and right-handed individuals are not specific to regions of interest. In particular, we found that  
13 connections between and within-hemispheres and the cerebellum show distinct patterns of  
14 connectivity. Together these results shed light on regions of the brain beyond those traditionally  
15 explored that contribute to differences in the functional organization of left- and right-handed  
16 individuals.

## 17 Introduction

18 Left-handed individuals comprise approximately 10% of the population<sup>1</sup>. This rare event in the  
19 population is believed to be due to the development of language lateralization in the left  
20 hemisphere, giving rise to a primarily right-handed population<sup>2</sup>. As such, the association  
21 between language lateralization and handedness have been well studied<sup>3,4</sup>. Additionally, brain  
22 differences between left- and right-handed individuals extend beyond language lateralization  
23 including differences in the motor and the somatosensory networks<sup>5,6</sup>. Neuroimaging studies  
24 have begun to highlight these differences using both functional activation<sup>7-10</sup> and  
25 morphometry<sup>11-13</sup>. Even so, these types of studies do not address how brain regions interact  
26 and, therefore, may give an incomplete picture of the brain correlates of handedness. Functional  
27 connectivity analysis using functional magnetic resonance imaging (fMRI) is a powerful tool to  
28 characterize group differences exhibiting temporal synchrony of activity among brain regions.  
29 While there have been some functional connectivity studies of handedness<sup>14-16</sup>, these are  
30 limited to specific networks chosen *a priori* and potentially fail to capture a complete picture of  
31 the connectivity profiles of handedness<sup>7-10</sup>.

32  
33 In this study, we utilize resting-state fMRI data, functional connectivity analyses, and cluster-  
34 based inference<sup>17</sup> to identify differences between left- and right-handed individuals using both  
35 hypothesis-based (e.g., networks of interest) and data-driven (e.g., whole-brain) approaches  
36 across two large datasets. For the hypothesis-based analyses, we define *a priori* networks of  
37 interest based on previous literature to investigate connectivity differences in the motor<sup>18</sup>,  
38 somatosensory<sup>6</sup>, and language<sup>19,20</sup> networks. For the data-driven analyses, we calculate whole-  
39 brain functional connectomes (i.e., a functional connectivity matrix containing pair-wise  
40 connections from all brain regions) using a 268-node functional brain parcellation<sup>21</sup>. As  
41 handedness preferences are well-established by 5 years of age<sup>22</sup>, we chose to investigate  
42 connectivity differences between left- and right-handed individuals using data from two  
43 developmental datasets<sup>23,24</sup>, the Healthy Brain Network (HBN) and the Philadelphia  
44 Neurodevelopmental Cohort (PNC). Because our sample contains school-aged children,  
45 adolescents, and young adults, we can better investigate innate differences in functional  
46 organization as opposed to the effects of adaptive differences caused by left-handed individuals  
47 interacting in environments typically designed for right-handed individuals.

48  
49 First, we performed cluster-based inference on our primary dataset, the HBN, establishing  
50 robust patterns of connectivity differences in the motor, somatosensory, and language networks.  
51 We then estimated the generalizability of these results to the PNC. Given the consistency of  
52 results and to increase power for whole-brain analyses, we combined these datasets to  
53 examine differences across the connectome and perform exploratory investigations of  
54 differences for within- and between-hemispheric edges, and cerebellar edges. Overall, these  
55 results demonstrate that wide-spread differences in functional organization, spanning the whole-  
56 brain, exist between left-handed and right-handed individuals. Thus, it may be important to  
57 account for handedness in functional connectivity studies, in particular for studies involving  
58 neuropsychiatric disorders, where left-handed individuals are disproportionately represented<sup>25</sup>.

59

## 60 Results

61 Data obtained from the Healthy Brain Network (HBN)<sup>23</sup> were used for the networks of interest  
 62 results. These networks of interest are based on previous literature that has shown functional  
 63 differences between left- and right-handed individuals. After excluding subjects for missing data  
 64 and excessive motion (>0.2mm), 905 individuals remain (right-handed: 787, left-handed: 118),  
 65 with ages ranging from 5-21 years. Edinburgh Handedness Questionnaire (EHQ) scores were  
 66 used as a measure of the extent individuals were left-handed and right-handed. For  
 67 generalization of networks of interest results, we used data from the Philadelphia  
 68 Neurodevelopmental Cohort (PNC)<sup>24,26</sup>. After excluding subjects for missing data and excessive  
 69 motion (>0.2mm), 859 subjects remain (right-handed: 742, left-handed: 117) with ages ranging  
 70 from 8-21 years. Measures of handedness were based on self-report of dominant hand in order  
 71 to complete a finger tapping task.

72  
 73 Resting-state fMRI data from both datasets were processed with identical, validated pipelines  
 74 and parcellated into 268 nodes (the Shen atlas) using a whole-brain, functional atlas defined  
 75 previously in a separate sample.<sup>21</sup> Next, the mean time courses of each node pair were  
 76 correlated and correlation coefficients were Fisher transformed, generating a connectome for  
 77 each participant. These connectomes were subsequently used in cluster-based inference, either  
 78 restricted to *a priori* networks of interest (i.e., motor, somatosensory, and language) or at the  
 79 whole-brain level. To define our networks of interest, we translated Brodmann areas from  
 80 previous literature onto the Shen atlas nodes (Table 1), visualizations of node allocations shown  
 81 in (Fig. S11). Handedness from the HBN was analyzed using EHQ scores as both continuous  
 82 values (when analyzing data from HBN independently) and as dichotomized data (when  
 83 combined with the PNC for data harmonization purposes). Only binary handedness data from  
 84 the PNC was available. Analyses were performed using the network-based statistic (NBS),  
 85 specifying a target familywise error rate of 5%.

86

Network	Brodmann Areas	Shen atlas nodes	
		Left	Right
Motor	<ul style="list-style-type: none"> <li>• Premotor/ Supp. motor: BA6<sup>27</sup></li> <li>• Primary Motor: BA4<sup>28</sup></li> </ul>	<ul style="list-style-type: none"> <li>• BA4: Node 158</li> <li>• BA6: Node 157, 159-166, 218</li> </ul>	<ul style="list-style-type: none"> <li>• BA4: Node 23</li> <li>• BA6: Node 24, 26, 27, 29-32</li> </ul>
Somatosensory	<ul style="list-style-type: none"> <li>• Primary Sensory: BA1<sup>29</sup></li> </ul>	<ul style="list-style-type: none"> <li>• BA1: Node 167, 171-173</li> </ul>	<ul style="list-style-type: none"> <li>• BA1: Node 33, 38-40</li> </ul>
Language: Broca's, Wernicke's	<ul style="list-style-type: none"> <li>• BA 44, BA9, BA 40<sup>8</sup></li> <li>• Wernicke's: BA22<sup>30</sup>, BA39<sup>31</sup></li> </ul>	<ul style="list-style-type: none"> <li>• BA9: Node 145-147</li> <li>• BA22: Node 197</li> <li>• BA39: Node 182-184</li> </ul>	<ul style="list-style-type: none"> <li>• BA9: Node 10, 11</li> <li>• BA22: Node 63, 64</li> <li>• BA39: Node</li> </ul>

	<ul style="list-style-type: none"> <li>• Broca's: BA44, BA45<sup>32</sup></li> </ul>	<ul style="list-style-type: none"> <li>• BA40: Node 179-181</li> <li>• BA44: Node 156</li> <li>• BA45: Node 155</li> </ul>	<p>48, 49</p> <ul style="list-style-type: none"> <li>• BA40: Node 45-47</li> <li>• BA44: Node 21, 22</li> <li>• BA45: Node 20</li> </ul>
--	--	--	--

87 **Table 1:** Allocation of nodes for each of the three networks of interest: motor, somatosensory, language. Node  
 88 definitions for both left and right hemispheres are based on Brodmann Areas as reported from previous literature of  
 89 differences in pure activation patterns.

90 Networks of Interest in HBN datasets

91 First, we examined the motor, somatosensory, and language networks in the HBN using EQ  
 92 as a continuous measure of handedness, where scores ranged from -100 (extremely left-  
 93 handed) to 100 (extremely right-handed). The network-based statistic<sup>17</sup> was used to identify  
 94 edges in a connectome that are significantly different between groups of individuals that are  
 95 primarily left-handed (left- > right-handed) and primarily right-handed (right- > left-handed).

96 *Motor*

97 Within the motor network (Fig. 1A/S1A), two clusters consisting of 227 edges (right- > left-  
 98 handed) and 195 edges (left- > right-handed) show significantly different ( $p < 0.05$ , two-tailed,  
 99 corrected) connectivity between groups. Interhemispheric connections between both sides of  
 100 the motor strip exhibited a mix of greater and weaker connectivity for the left- > right-handed  
 101 group compared to right- > left-handed group. However, edges between the motor areas and  
 102 other regions of the brain show distinct patterns between the left- > right-handed group and  
 103 right- > left-handed group. In the right- > left-handed group, edges of greater connectivity  
 104 compared to left-handed individuals are scattered throughout the brain across all anatomical  
 105 regions. Notably, the majority of these edges are between-hemisphere edges relative to within-  
 106 hemispheres (between: (136/227 edges or 59.9%; within: 91/227 edges or 40.0%;  $\chi^2 = 4.31$ ,  
 107  $p = 0.038$ ; Fig. S2).

108  
 109 In contrast, a majority of edges showing greater in the left-> right-handed groups are within-  
 110 hemisphere edges with between-hemisphere generally being confined to motor-motor edges  
 111 (between: 82/195 edges or 42.0%; within: 113/195 edges or 58.0%;  $\chi^2 = 2.64$ ,  $p = 0.104$ ; Fig. S2).  
 112 Neither group exhibit edges confined to a specific hemisphere (left- > right-handed:  $\chi^2 = 1.79$ ,  
 113  $p = 0.181$ ; right- > left-handed:  $\chi^2 = 1.42$ ,  $p = 0.233$ ; Fig. S2). Perhaps most interestingly, we  
 114 observe a bundle of edges between the right motorstrip and the ipsilateral cerebellum in left-  
 115 handed individuals, in alignment with the known roles for the cerebellum in motor control and  
 116 adjustments<sup>33</sup>. Yet, canonical motor-cerebellar circuits point towards contralateral connections  
 117 (i.e., the right motor strip connects to the left cerebellum). That we observed stronger ipsilateral  
 118 functional connections in left-handed individuals may point toward neuroplasticity of left-handed  
 119 individuals needing to adapt to a primarily right-dominant society (e.g., scissors, computer  
 120 mice)<sup>34</sup>.

## 121 *Somatosensory*

122 Similar patterns are observed for the somatosensory network (Fig. 1B/S1B) with two clusters  
123 consisting of 127 edges (right- > left-handed) and 88 edges (left- > right-handed) exhibiting  
124 significantly different ( $p < 0.05$ , corrected) connectivity between left- > right-handed and right- >  
125 left-handed groups. Neither group exhibit edges lateralized to specific hemisphere (left-> right-  
126 handed:  $\chi^2 = 2.22$ ,  $p = 0.136$ ; right- > left-handed:  $\chi^2 = 0.04$ ,  $p = 0.841$ ; Fig. S2). For edges of  
127 greater connectivity in right-handed individuals, a majority are between-hemisphere edges  
128 relative to within-hemispheres (between: 80/127 edges or 63.0%; within: 37/127 edges or  
129 37.0%;  $\chi^2 = 7.81$ ,  $p = 0.005$ ; Fig. S2).

130  
131 For edges of greater connectivity in the left- > right-handed group, a majority are within-  
132 hemisphere edges relative to between-hemispheres (between: 29/88 edges or 33.0%; within:  
133 59/88 edges or 67.0%;  $\chi^2 = 5.27$ ,  $p = 0.022$ ; Fig. S2). However, of the contralateral edges  
134 identified as greater connectivity in the left- > right-handed group, the majority are edges  
135 stemming from the parietal networks to the contralateral cerebellum on both sides. This could  
136 be partly due to the previous phenomena explained in the motor network. Studies have also  
137 shown that the cerebellum has representation of somatosensory<sup>35</sup>, accounting for the  
138 synchronous activity observed in both populations, but particularly in left-handed individuals.

## 139 *Language*

140 Finally, for the language network (Fig. 1C/S1C), two clusters consisting of 337 edges (right- >  
141 left-handed) and 325 edges (left- > right-handed) display significantly different ( $p < 0.05$ ,  
142 corrected) connectivity between left- > right-handed and right- > left-handed groups. Similarly to  
143 the patterns observed in the motor and somatosensory networks, the connectivity of cerebellum  
144 is notable. Bundles of edges, exhibiting greater connectivity in the left- > right-handed group,  
145 between both frontal lobes to the ipsilateral cerebellum are present. Additionally, bundles of  
146 edges with greater connectivity in right-handed individuals are observable between nodes in the  
147 right parietal lobe and both hemispheres of the cerebellum.

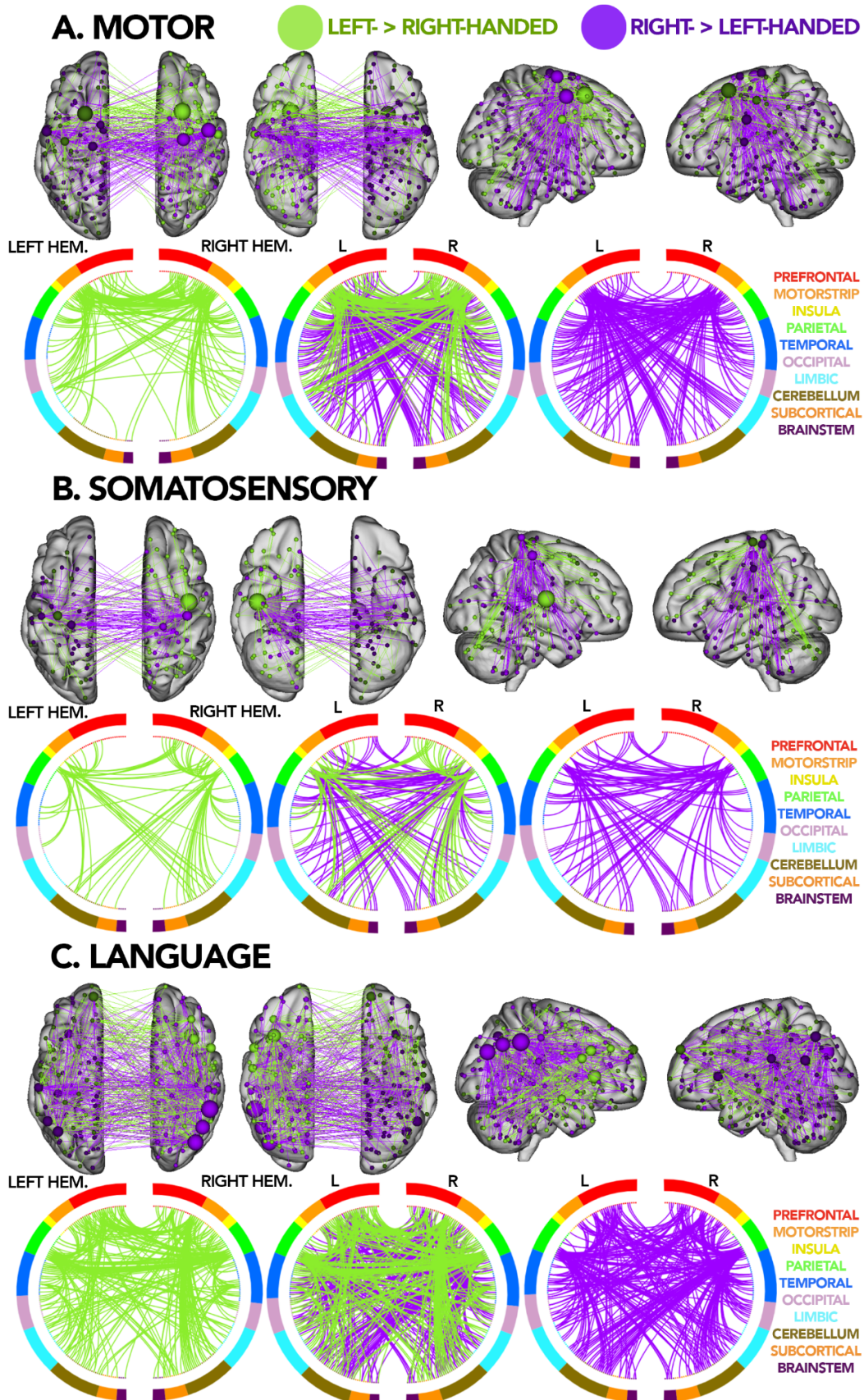
148  
149 In contrast to the motor and somatosensory networks, no differences in the distribution of  
150 between and within-hemisphere edges in the right- > left-handed group is observed (between:  
151 165/337 edges or 49.0%; within: 172/337 edges or 51.0%;  $\chi^2 = 0.05$ ,  $p = 0.823$ ; Fig. S2).

152 However, similar to the motor and somatosensory networks, a majority of edges exhibiting  
153 greater connectivity in the left- > right-handed group are within-hemisphere edges relative to  
154 between-hemispheres (between: 133/325 edges or 40.9%; within: 192/325 edges or 59.1%;  
155  $\chi^2 = 5.22$ ,  $p = 0.022$ ; Fig. S2) with between-hemisphere edges primary located between the  
156 parietal lobes. Neither group exhibit edges lateralized to specific hemisphere (left-handed:  
157  $\chi^2 = 3.40$ ,  $p = 0.065$ ; right-handed:  $\chi^2 = 1.17$ ,  $p = 0.279$ ; Fig. S2).

158  
159 We observe that nodes with the largest number of significantly greater edges for right-handed  
160 individuals (*i.e.*, hubs) are located in both parietal lobes. Surprisingly, given the lateralization of  
161 language to the left hemisphere in the right- > left-handed group, the largest hubs are located in  
162 the secondary language regions in the right parietal lobe. In contrast, the left- > right-handed

163 group shows hubs of significantly greater connectivity in the right hemisphere homologue of  
164 Broca's area<sup>36</sup>. Overall, while the right- > left-handed group showed more widespread  
165 connectivity throughout the language networks, these edges appear to form hubs in the parietal  
166 lobe. Additionally, the cerebellum is differentially connected to the language network between  
167 groups. In particular, frontal-cerebellar connections were more prominent for the left- > right-  
168 handed group and parietal-cerebellar connections more prominent for the right- > left-handed  
169 group.

170  
171 For all networks of interest, results yielded similar results when using the EHQ as a continuous  
172 or binary variable (EHQ < 0 = left-handed individuals, EHQ > 0 = right-handed individuals) (Fig.  
173 S3) and controlling for various demographic factors (e.g., age, sex) (Tables S1-S6). Overall,  
174 these results build upon previous work showing differences in activation patterns in networks of  
175 interest such that these differences are also observable in patterns of connectivity for all  
176 networks of interest.





178 **Fig. 1:** Brain and circle plots for each of the a priori defined networks in the HBN dataset. Edges that are greater for  
179 the left- > right-handed group are shown in green while edges that are greater for the right > left-handed group are  
180 shown in purple. Top row for each section shows significant edges drawn on an anatomical 3D brain with nodes sized  
181 based on the number of significant edges identified. Bottom row for each section shows circle plots where the left and  
182 right hemispheres are depicted as left and right semi-circles, respectively. The middle circle plot shows an overlay  
183 between left- and right-handed individuals. Nodes are color-coded by anatomical region constructed based on the  
184 Shen atlas, each line depicts a significant edge identified through NBS. Legend for which anatomical region each  
185 color represents is shown next to the circle plots. Each section shows results for each network of interest: (A) motor  
186 (p-val: 0.027), (B) somatosensory (p-val: 0.024), (C) language (p-val: 0.005).

## 187 Generalization of networks of interest results to the PNC dataset

188 Using the network of interest approach, we then looked at how well these results based on data  
189 from the HBN generalized to other datasets of similar populations using data from the PNC (Fig.  
190 S4). We observed similar patterns of group differences in the HBN and PNC datasets as  
191 evidenced by the number of overlapping edges and the correlation of nodal degree between the  
192 two sets of results. First, using the hypergeometric cumulative density function to determine  
193 significance of the edge-level overlap between two networks<sup>37</sup>, all resulting networks of group  
194 differences were significant between the two analyses (p<0.05; Fig. S5: top row) with the  
195 exception of the network of greater edges for the left- > right-handed group in the motor  
196 network. Second, for each network of group differences, node degree--defined as the number of  
197 significant edges for each node--was calculated and correlated between the HBN and PNC  
198 results. All result pairs showed a significant correlation between nodal degree (all r's>0.54, all  
199 p's<0.001). Quantitatively, in the motor network, a fraction of the edges connecting the right  
200 motorstrip and ipsilateral cerebellum are present in the PNC as well. Whereas in the  
201 somatosensory network, similar crossing patterns connecting somatosensory nodes with  
202 contralateral cerebellum nodes are observed. Overlapping edges in the language network  
203 continue to highlight the importance of the cerebellum in connectivity differences between the  
204 left- > right-handed and right- > left-handed groups. Notably, the measures of handedness  
205 between the HBN and PNC were conducted differently as the HBN utilized EHQ scores which  
206 ranged from -100 to 100 while the PNC was based on self-reported measures of dominant hand  
207 for a hand tapping task. Despite differences in behavioral measures, similar patterns of  
208 connectivity were repeatedly identified as significantly different between the left- > right-handed  
209 and right- > left-handed groups. This highlights the robustness and generalizability of these  
210 results.

## 211 Whole-brain analysis: HBN + PNC

212 After having established that observed differences between the left- > right-handed and right- >  
213 left-handed groups in the HBN generalize to the PNC, we combined the two datasets to  
214 increase our sample size and statistical power for whole brain analyses. To harmonize the  
215 handedness measures in the HBN and PNC, we binarized the EHQ scores to make them  
216 consistent with the PNC, such that individuals with a score below 0 were classified as primarily  
217 left-handed (left- > right-handed) and individuals with a score above 0 were classified as  
218 primarily right-handed (right- > left-handed).

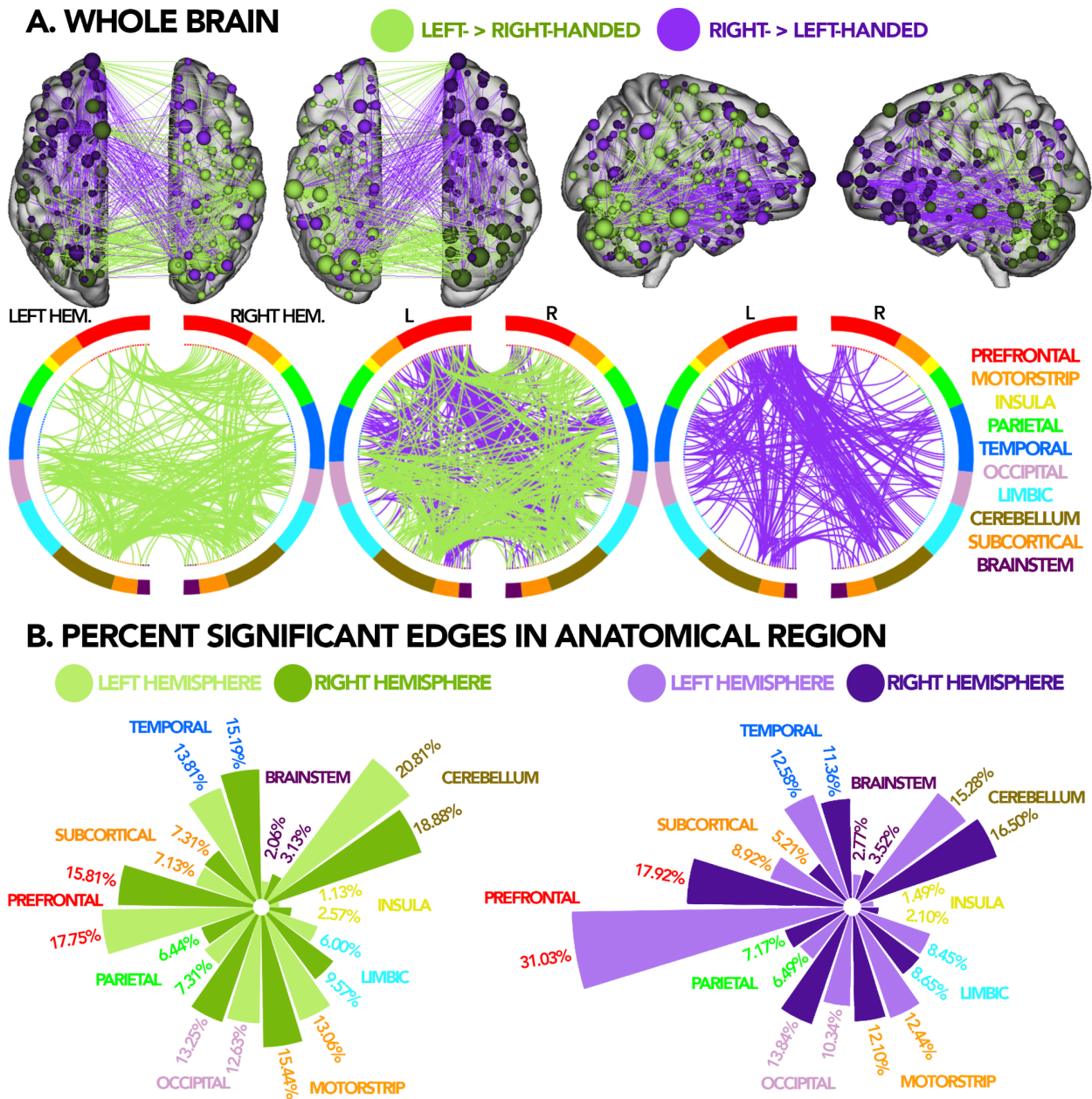
219

220 Despite previous literature, widespread connectivity was observed across the whole brain  
221 between the left- > right-handed and right- > left-handed groups at the level of the whole brain  
222 (Figs. 2A & S6), beyond those in the networks of interest. Two clusters consisting of 1600 edges  
223 (right- > left-handed) and 1450 edges (left- > right-handed) exhibit significantly different ( $p < 0.05$ ,  
224 corrected) connectivity between the two groups. Similar to the networks of interest analyses,  
225 cerebellar connections are prominent (left- > right-handed: 39.69% significant edges, right- >  
226 left-handed: 31.78% significant edges; Fig. 2B). We observe a large proportion of edges  
227 exhibiting greater connectivity for the right- > left-handed group between the right cerebellum  
228 and the left prefrontal regions. In contrast, edges of greater connectivity for the left- > right-  
229 handed group were more localized to connections between the cerebellum and posterior  
230 regions (e.g., the occipital and parietal lobes). Results are similar when controlling for various  
231 demographic factors (e.g., age and sex for both HBN and PNC; scan sites and clinical  
232 diagnoses for HBN) (Tables. S14-S19).

233  
234 Edges of greater connectivity for the right- > left-handed group were more *lateralized* within the  
235 left hemisphere (within left hemisphere: 423 edges; within right hemisphere: 324 edges;  $\chi^2 = 6.46$ ,  
236  $p = 0.011$ ; Fig. S7), consistent with the theory of left-hemisphere dominance in right-handed  
237 individuals<sup>38</sup>. However, edges of greater connectivity for the left- > right-handed group were not  
238 *lateralized* to either hemisphere (within left hemisphere: 353 edges; within right hemisphere: 411  
239 edges;  $\chi^2 = 2.20$ ,  $p = 0.138$ ; Fig. S7), consistent with the observation of a mix of left- and right-  
240 hemisphere dominance, or even right-hemisphere dominance, in the left- > right-handed group.  
241 No differences in the distribution of between and within-hemisphere edges in left- or right-  
242 handed individuals are observed (left- > right-handed between: 836/1600 edges or 52.3%;  
243 within: 764/1600 edges or 47.8%;  $\chi^2 = 1.62$ ,  $p = 0.203$ ; right- > left-handed between: 732/1450  
244 edges or 49.8%; within: 737/1450 edges or 50.2%;  $\chi^2 = 0.01$ ,  $p = 0.920$ ; Fig. S7).

245  
246 The largest proportion of edges that differed between left- and right-handed individuals were  
247 localized to the prefrontal lobe (left- > right-handed: 33.56% significant edges, right- > left-  
248 handed: 48.93% significant edges; Fig. 2B), consistent with our network of interest results,  
249 where expressive language processing nodes (e.g., Broca's region) and secondary motor nodes  
250 are located. Surprisingly, but in line with Fig. 2A, the cerebellum contained the second largest  
251 amount of edges that differed between the left- > right-handed and right- > left-handed groups  
252 (left- > right-handed: 39.69% significant edges, right- > left-handed: 31.78% significant edges;  
253 Fig. 2B). These results were consistent when normalizing the number of edges within each  
254 network (Fig. S8). Of the 3079 edges that were identified as significantly different between the  
255 two groups at the whole-brain level, only 16.95% were also initially identified as significant using  
256 the networks of interest analysis. Overall, this observation suggests that functional connectivity  
257 differences between left- and right-handed individuals span the whole brain--rather than being  
258 localized to specific networks as suggested by previous literature<sup>4,6</sup>.

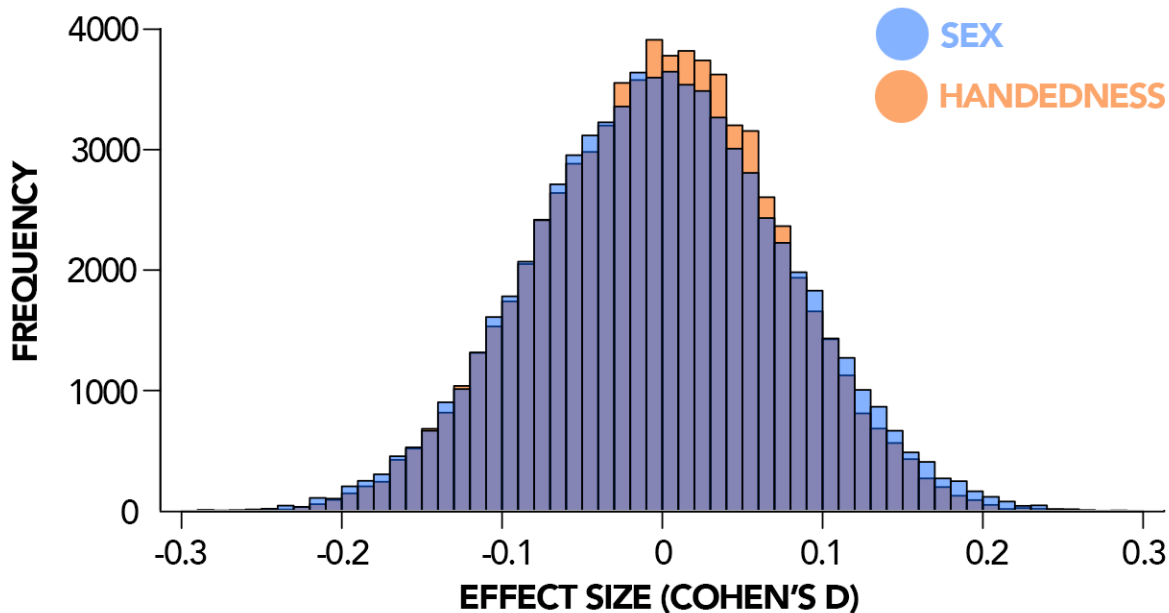
259



260  
 261 **Fig. 2:** (A) Brain and circle plots for the entire connectome ( $p\text{-val} = 0.0018$ ), circle plots and brain plots were  
 262 thresholded at a degree threshold of 50 for visualization. Results for the left- > right-handed group are shown in green  
 263 while results for the right- > left-handed group are shown in purple. Top row for each section shows significant edges  
 264 drawn on an anatomical brain with nodes sized based on the number of significant edges identified. Bottom row  
 265 shows circle plots where the left and right hemispheres are depicted as left and right semi-circles, respectively. The  
 266 middle circle plot shows an overlay between groups. Nodes are color-coded by anatomical regions constructed based  
 267 on the Shen atlas, each line depicts a significant edge identified through NBS. (B) Circular bar graph quantifying the  
 268 percent of significant edges in each anatomical network corresponding with the circle plots in 2A split by left and right  
 269 hemispheres, for left- > right-handed and right- > left-handed groups.

270  
 271 Next, we quantified the effect size via Cohen's D of the connectivity differences between left-  
 272 and right-handed individuals for all edges. These effect sizes ranged from -0.3 to 0.3, consistent  
 273 with the observation that brain-behavior associations tend to have low to medium effect

274 sizes<sup>39,40</sup>. To help put these whole-brain differences into comparable context relative to sex  
275 differences, for primarily right-handed individuals only, we compared the connectomes between  
276 male and females participants (based on self-reported sex) and quantified edgewise effects  
277 sizes for these differences. Broadly, the effect sizes observed for sex differences in whole-brain  
278 functional connectivity were of a similar magnitude as the effect sizes observed for handedness  
279 differences (Fig. 3) with no significant differences between the two distributions of effect-sizes  
280 being observed. Together, these results suggest that handedness differences account for a  
281 similar amount of individual differences in the connectome as sex differences, and underscore  
282 that the handedness effects are neurobiologically meaningful in addition to being statistically  
283 significant.  
284



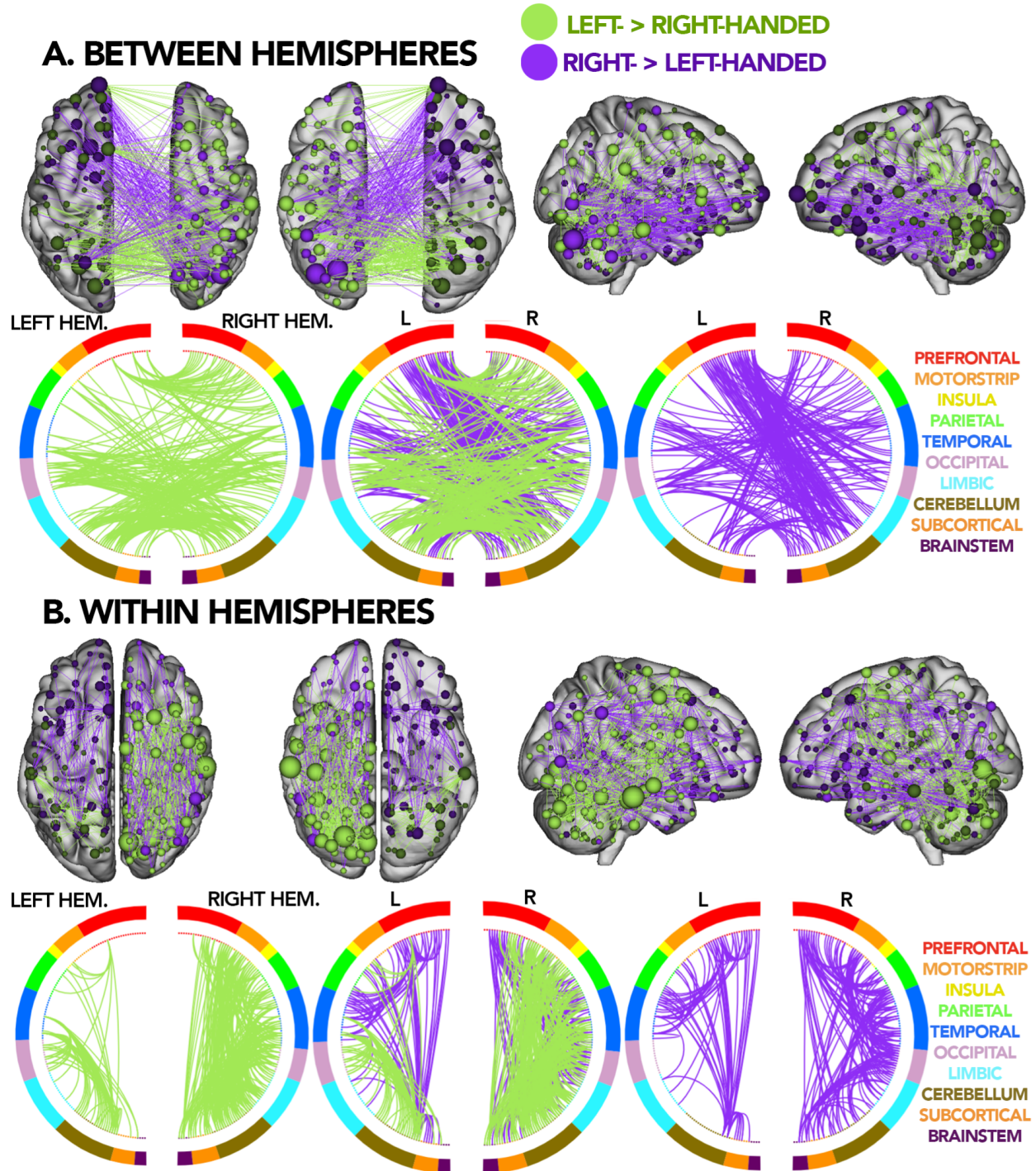
285  
286 **Fig. 3:** Comparison of effect sizes for each edge in a connectome (total 35,778 edges) plotted onto a histogram for  
287 handedness and sex.

### 288 Between and within hemispheres

289 Analyses on between-hemisphere edges (Fig. 4A) demonstrate very similar patterns to those of  
290 the whole brain. The same bundles of edges forming between the left prefrontal and  
291 contralateral cerebellum make up the majority of between-hemisphere edges that are  
292 significantly greater for the right- > left-handed group. Similarly, the same patterns of cerebellar  
293 edges for the left- > right-handed group is observed in our between-hemisphere analyses.  
294 Overall, cerebellar edges make up the majority of significant between-hemisphere edges when  
295 comparing the two groups (1108/1568 edges or 70.7%).

296  
297 The within-hemisphere results show diverging *laterality* patterns from our whole-brain analyses  
298 (Fig. 4B). Consistent with the whole-brain results, edges of greater connectivity for the right- >  
299 left-handed group were more *lateralized* within the left hemisphere (within left hemisphere: 423  
300 edges; within right hemisphere: edges: 324;  $\chi^2=6.46$ ,  $p=0.01$ ). However, edges of greater  
301 connectivity for the left- > right-handed group were more *lateralized* within the right hemisphere

302 for within-hemisphere edges (within left hemisphere: 324 edges; within right hemisphere: 821  
303 edges;  $\chi^2=97.4$ ,  $p<0.001$ ). This finding is in contrast to our whole-brain results, where the left- >  
304 right-handed group exhibited a non-significant lateralization to the right hemisphere. Perhaps,  
305 given the more localized analysis to only within-hemisphere, the null clusters from the  
306 permutation analysis were smaller, leading to additional information surviving NBS correction. In  
307 other words, by restricting our analysis, we were able to see better under the spotlight<sup>43</sup>.  
308 Together, these results are consistent with the observation of left-hemisphere dominance in  
309 primarily right-handed individuals and mixed or right-hemisphere dominance in primarily left-  
310 handed individuals<sup>4,44</sup>.



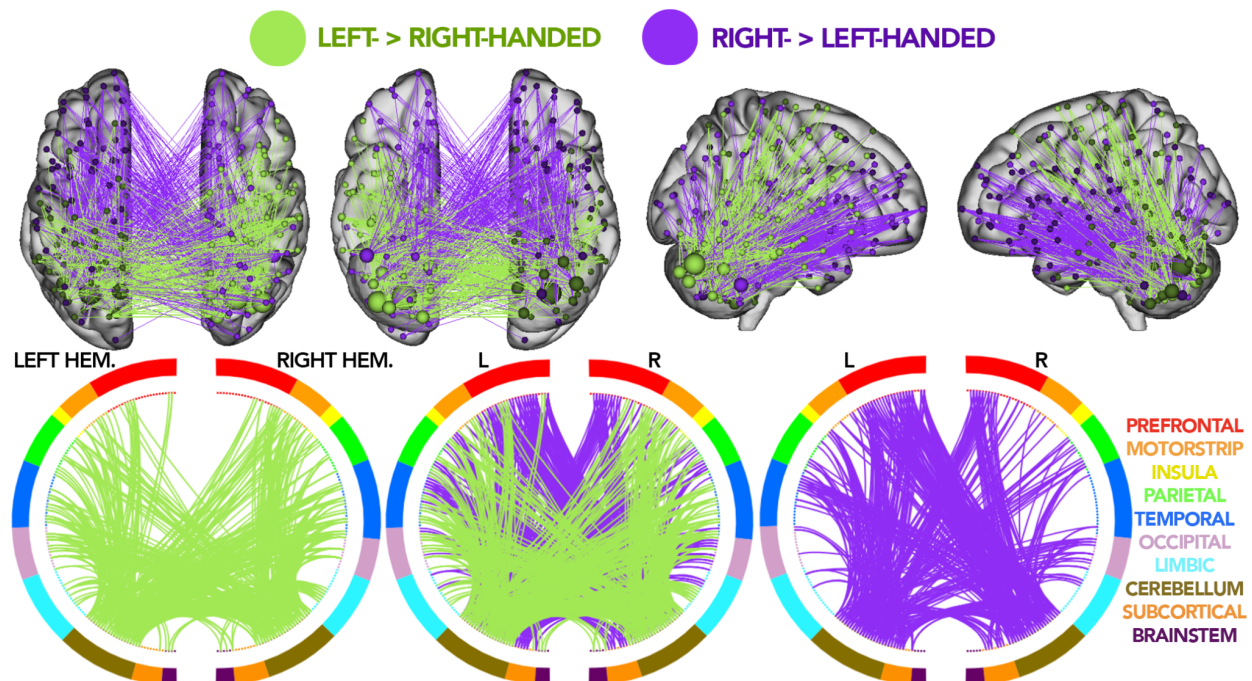
311  
312 **Fig. 4:** (A) Brain and circle plots for significant edges between-hemispheres ( $p = 0.012$ ), circle plots and brain plots  
313 were thresholded at a degree threshold of 25 for visualization. (B) Brain and circle plots for significant edges for  
314 within-hemispheres (left hemisphere  $p = 0.019$ , right hemisphere  $p = 0.022$ ), circle plots and brain plots were  
315 thresholded at a degree threshold of 25 for visualization. Results for the left- > right-handed group are shown in green  
316 while results for the right- > left-handed group are shown in purple. Top row for each section shows significant edges  
317 drawn on an anatomical brain with nodes sized based on the number of significant edges identified. Bottom row for  
318 each section shows circle plots where the left and right hemispheres are depicted as left and right semi-circles,  
319 respectively. The middle circle plot shows an overlay of circle plots for both groups. Nodes are color-coded by data-  
320 driven networks constructed based on the Shen atlas, each line depicts a significant edge identified through NBS.

## 321 Cerebellum

322 Given the striking contribution of the cerebellum to the network of interest (Fig. 1) and whole-  
323 brain group differences (Figs. 2 & 4) as well as the relatively unexplored functional differences in  
324 the cerebellum between the left- > right-handed and right- > left-handed groups<sup>45</sup>, we further  
325 investigated cerebellar differences in functional connectivity using our networks of interest  
326 approach.

327  
328 Within the cerebellar network (Fig. 5), clusters consisting of 463 edges (right- > left-handed) and  
329 558 edges (left- > right-handed) exhibit significantly different ( $p < 0.05$ , corrected) connectivity  
330 between the left- > right-handed and right- > left-handed groups. The left- > right-handed group  
331 show large bundles of edges with significantly greater connectivity between the cerebellum and  
332 the motor strip and somatosensory areas, consistent with results for the motor and language  
333 networks (Fig. 1). Interestingly, edges of greater connectivity for the left- > right-handed group  
334 are generally confined towards the posterior regions of the brain whereas edges of greater  
335 connectivity for the right- > left-handed group are generally confined to the frontal regions.  
336 Results are similar when controlling for various demographic factors (e.g., age, sex) (Tables.  
337 S1-S4). Edges of greater connectivity in the right- > left-handed group are mostly between-  
338 hemisphere edges rather than within hemispheres (between: 274/463 edges or 59.2%; within:  
339 189/463 edges or 40.8%;  $\chi^2 = 7.69$ ,  $p = 0.006$ ; Fig. S12) and are more *lateralized* within the left  
340 hemisphere (within left hemisphere: 126 edges; within right hemisphere: 63 edges;  $\chi^2 = 14.86$ ,  
341  $p < 0.001$ ; Fig. S12). No differences in the distribution of edges of greater connectivity in the left-  
342 > right-handed group were observed (between: 284/558 edges or 50.9%; within: 274/558 edges  
343 or 49.1%;  $\chi^2 = 0.09$ ,  $p = 0.76$ ; within left hemisphere: 132 edges; within right hemisphere: 152  
344 edges;  $\chi^2 = 0.71$ ,  $p = 0.40$ ; Fig. S12).

345



347 **Fig. 5:** Brain and circle plots for all nodes in the cerebellum ( $p\text{-val} = 0.031$ ). Results for the left- > right-handed group  
348 are shown in green while results for the right- > left-handed group are shown in purple. Top row shows significant  
349 edges drawn on an anatomical brain with nodes sized based on the number of significant edges identified. Bottom  
350 row shows circle plots where the left and right hemispheres are depicted as left and right semi-circles, respectively.  
351 The middle circle plot shows an overlay between left- and right-handed individuals. Nodes are color-coded by data-  
352 driven networks constructed based on the Shen atlas, each line depicts a significant edge identified through NBS.  
353



## 354 Discussion

355 Using functional connectomes from two large open-source datasets (the Healthy Brain Network  
356 and Philadelphia Neurodevelopmental Cohort), we show that differences in the functional  
357 organization between groups of primarily left- and primarily right-handed individuals are found  
358 not only in previously identified functional networks, but in every brain region with a strikingly  
359 large amount of differences for edges incident to the cerebellum. We began by investigating  
360 differences in networks of interest, as established by previous activation studies, to show that  
361 these differences can also be detected by functional connectivity. These differences also  
362 robustly generalized across datasets. In a combined sample from both datasets, we show that  
363 differences in functional connectivity between the left- > right-handed and right- > left-handed  
364 groups are present across the whole brain. In particular, to emphasize the significance of these  
365 differences, we compared the distribution of effect sizes to those from self-reported sex.  
366 Handedness differences exhibit similar effect sizes as sex differences suggesting handedness  
367 may be a factor researchers should control for in future large-scale connectome studies. Finally,  
368 while previous studies have focused on the cortex<sup>28,46</sup>, we find that the most striking differences  
369 between the left- > right-handed and right- > left-handed groups are edges located within and  
370 between the cerebellum. Together, these results characterize fundamental differences in the  
371 functional connectome associated with handedness.

### 372 Whole brain analyses: going beyond regions of interest

373 Deviating from traditional region and network of interest approaches, our whole-brain results  
374 emphasize that differences between the left- > right-handed and right- > left-handed groups are  
375 wide-spread across the whole brain rather than localized to a few regions and networks. Indeed,  
376 only 16.95% of edges from the whole-brain results were identified as significant using the  
377 networks of interest analysis. The widespread nature of our results is also in contrast to  
378 emerging morphometric studies of handedness, which similarly report sparse, localized  
379 differences between the two groups<sup>47</sup>. A potential explanation may be that functional  
380 connections have greater neuroplasticity than anatomical structures<sup>34</sup>. Given the relative rarity  
381 of left-handed individuals (approximately 10% of the population<sup>48</sup>), they may be forced to use  
382 tools designed for right-handed individuals (e.g., scissors or computer mouse). This adaptation  
383 likely results in neuroplasticity with large-scale changes in functional connectivity, likely not  
384 observable in fixed anatomical structures.

### 385 Cerebellum

386 Despite a majority of handedness work focusing on the cortex<sup>2,28,32,49-52</sup>, the cerebellum  
387 demonstrated the second largest number of significant edges of networks evaluated in the data-  
388 driven, whole-brain analysis (the prefrontal lobe, which includes several of our networks of  
389 interest, contained the largest number of significant edges). Reported associations between  
390 handedness and the cerebellum are limited<sup>13,45</sup>. Perhaps this result is not surprising given the  
391 cerebellum's role in motor control<sup>53,54</sup> and the association of motor control and handedness<sup>28,49</sup>.  
392 Nevertheless, most of the significant edges do not involve the motor cortex, in line with the  
393 recent trend to consider the cerebellum as a cognitive region, rather than a solely motor

394 region<sup>55</sup>. The cerebellum develops rapidly postnatally<sup>56</sup>, during a time when infants acquire a  
395 vast amount of skills and handedness begins to crystalize. As periods of rapid development  
396 show the greatest neuroplasticity<sup>34</sup>, it may be reasonable to expect that functional connections  
397 are more plastic in the cerebellum than other regions, resulting in the large functional  
398 differences in the cerebellum.

#### 399 Effect sizes: controlling for handedness in large studies

400 Given the magnitude of effect sizes in neuroimaging and clinical and social factors associated  
401 with sex differences<sup>57</sup>, sex is routinely controlled for in neuroimaging studies<sup>58,59</sup>. The similarity  
402 between the effect size magnitude of handedness differences and sex differences in FC  
403 underscores the importance of potentially accounting these functional differences. Future  
404 studies that include a large number of left-handed individuals may need to control for  
405 handedness in a similar manner as other covariates, such as sex. One caveat might be that left-  
406 handed individuals are relatively rare (around 10% of the population<sup>1</sup>). Many functional  
407 connectivity studies may not have a sufficiently large sample of left-handed individuals to  
408 properly estimate these effects. However, potential differences in the connectome should not be  
409 used to justify excluding left-handed individuals from a study. Best practices in maintaining  
410 representative samples necessitates the inclusion of left-handed individuals<sup>60</sup>. Nevertheless, the  
411 best approach for accounting for handedness differences in the connectome remains to be  
412 determined.

#### 413 Functional connectivity relative to other brain studies of handedness

414 In line with previous results from activation, morphometric, neuropsychological, and lesion<sup>61</sup>  
415 studies, we found that functional connectivity incident to the motor, somatosensory, and  
416 language networks differed between primarily left- and primarily right-handed individuals. While  
417 our results build upon this previous work, differences in functional connectivity do not  
418 necessarily translate to observed differences in brain activation<sup>62</sup> or structure. For instance, one  
419 may expect large functional connectivity differences in Broca's and Wernicke's areas<sup>3,32</sup> based  
420 on previous work in activation studies regarding lateralization differences in language between  
421 left- and right-handed individuals. Yet, we found the largest number of significantly different  
422 edges clustered in the right-hemisphere, located in secondary language processing regions of  
423 the temporoparietal junction (in the right- > left-handed group). The lack of one-to-one  
424 translation of results between functional connectivity and activation likely holds in the other  
425 direction, too. In other words, the lack of differences in functional connectivity does not imply  
426 that activation patterns in Broca's or Wernicke's areas between the left- > right-handed and  
427 right- > left-handed groups during a language task would be the same. Patterns of within- and  
428 between-hemisphere edges also appear to be consistent across all three networks.

#### 429 Lateralization/cross hemispheric connections

430 Additionally, while little lateralization was observed using the network of interest, strong  
431 lateralization effects were observed in the whole-brain results, consistent with patterns of left

432 hemisphere dominance in right-handed individuals<sup>44,63</sup>. As such, we delved deeper into  
433 analyzing patterns of connectivity for significant edges within and between hemispheres. We  
434 consistently observe a greater amount of within-hemisphere edges for the left- > right-handed  
435 group whereas we observe a greater amount of between-hemisphere edges for the right- > left-  
436 handed group. These differences in between and within-hemisphere edges could result from  
437 differences in corpus callosum connectivity associated with handedness. Differences in the  
438 amount of between-hemispheric connections via the corpus callosum has been shown to be  
439 linked to the extent of handedness an individual exhibits<sup>7</sup> (i.e., the more ambidextrous an  
440 individual, the more connections between hemispheres). Overall, these observations highlight  
441 that handedness differences in the functional connectome are vastly more distributed than  
442 previously understood.

#### 443 Strengths and weaknesses

444 There are several notable strengths of our study. First, we used two large open-source  
445 datasets, allowing for a large sample of left-handed individuals ( $n > 225$ ), the application of  
446 whole-brain approaches and the ability to investigate generalization/replication of results across  
447 study designs. Without the large sample size and whole-brain analyses, important results (e.g.,  
448 the widespread nature of handedness differences and the large handedness differences in  
449 cerebellum) may not have been discovered. Similarly, generalizing results from the HBN to the  
450 PNC highlight their robustness, especially considering the different handedness measures  
451 across the datasets. Second, by focusing on school-age children and adolescents as opposed  
452 to adults, we can better investigate the innate differences in connectivity, rather than adaptive  
453 differences acquired over the course of life. For example, historically, left-handed individuals  
454 were often forced to write right-handed. Also cultural stigma may have led others to become  
455 functionally right-handed<sup>64</sup> (e.g., sinister means both evil and left). Yet, even in a younger  
456 sample, fully ruling out adaptive differences is not possible.

457  
458 Nevertheless, there are several notable limitations of our study. First, while all of our analyses  
459 are based on the same procedure and thresholds using NBS, it is important to note that running  
460 NBS on a subsetting connectome as opposed to the whole connectome will select different  
461 edges as a result. For instance, an edge that is initially identified as significant based on a  
462 subsetting connectome (like in our networks of interest) may not be identified as significant when  
463 using the entire connectome. Second, in defining our networks of interest, we based our  
464 definitions on differences in activation patterns shown in previous studies<sup>6,8,65</sup>. These previous  
465 studies have typically reported their results in the context of Brodmann areas, where our  
466 connectomes are parcellated based on a 268-node functionally defined atlas. Thus, we  
467 manually identified nodes that overlapped with these Brodmann areas, however, due to the  
468 differences in the Shen atlas and the Brodmann areas, our networks of interest may not have  
469 captured the exact regions that were reported in previous studies. Moreover, the Brodmann  
470 atlas is symmetrical between hemispheres, while our 268-node atlas is not. As such, there are  
471 also asymmetries between areas of the brain included in our analyses of networks of interest  
472 between the left and right hemispheres. Third, in our whole-brain analysis, we were limited to  
473 binarizing the EHQ in the HBN datasets for harmonization with the PNC handedness measure.  
474 While we could have explored a third group of ambidextrous individuals in HBN, we were limited

475 by: (a) the fact that there is no gold standard for the range of scores in the EHQ to classify an  
476 ambidextrous group<sup>66</sup> and (b) the PNC's measures of handedness was a forced-choice self  
477 report of handedness. Because of the variability and range in EHQ scores, we chose to conduct  
478 our initial analyses on the HBN and subsequent generalization/harmonization to the PNC.  
479 Finally, to address handedness interactions with sex and age, we repeated all NBS analyses  
480 using partial correlation to control for these factors (sex: Table S1, age: Table S3) as well  
481 conducting combined analyses for the two datasets separately (sex: Table S2, age Table S4).  
482 These results robustly demonstrate that while sex and age are potential confounding factors,  
483 our results remain unchanged as the same significant edges are identified with and without  
484 controlling for these factors. Additionally, we also controlled for scanning site and clinical  
485 diagnoses for the HBN, since this population was scanned across multiple sites and contained  
486 many subjects with clinical diagnoses (site: Table S5, diagnoses: Table S6). Similarly, the same  
487 significant edges were robustly identified as significant with or without controlling for scanning  
488 site and clinical diagnoses.

#### 489 Future directions

490 In sum, we show that differences in the functional connectome associated with handedness are  
491 distributed across the brain, including previously unreported differences associated with the  
492 cerebellar network. Future directions include investigations into sex-handedness  
493 interaction<sup>11,28,67,68</sup> (as majority of left-handed population consists of males<sup>48</sup>), into a third  
494 ambidextrous group, and into potential interactions between handedness and psychiatric  
495 diagnoses (as non-right handedness is overrepresented in various psychiatric disorders, namely  
496 schizophrenia<sup>25</sup>). As the observed differences show meaningful effect sizes, future studies may  
497 need to consider accounting for handedness. This work serves as a starting point to account for  
498 handedness in functional connectivity studies, in particular for studies involving neuropsychiatric  
499 disorders.  
500

## 501 **Methods**

### 502 Dataset: HBN

503 All connectomes for initial analyses (Fig. 1) were generated from resting-state scans obtained  
504 from the Healthy Brain Network (HBN)<sup>23</sup>. All resting-state scans are 10 mins long using a 1.5 T  
505 Siemens Avanto system equipped with 45 mT/m gradients in a mobile trailer at four different  
506 sites around the New York greater metropolitan area: Staten Island, Cornell University, City  
507 University of New York, and Rutgers University. After excluding subjects for missing scans/data  
508 and excessive motion (>0.2 mm), 905 subjects remain (right- > left-handed group: 787, left- >  
509 right-handed individuals: 118). Subjects' ages ranged from 5-22 where 111 subjects had no  
510 diagnosis and 794 had some diagnosis of learning disorders or symptoms of psychiatry.  
511 Edinburgh Handedness Questionnaire scores were used as a measure of the extent subjects  
512 were left-handed and right-handed. Scores ranged from -100 to 100 where -100 is considered  
513 an extremely left-handed individual and 100 is considered an extremely right-handed individual.

### 514 Dataset: PNC

515 For generalization, we used data from the Philadelphia Neurodevelopmental Cohort (PNC)<sup>24,26</sup>  
516 by following the same preprocessing pipelines used with HBN. All resting-state scans are 6  
517 mins long using a single 3T Siemens TIM Trio whole-body scanner with the VB17 revision of the  
518 Siemens software. All participants were scanned at the University of Pennsylvania in  
519 Philadelphia, PA. After excluding subjects for missing scans/data and excessive motion (>0.2  
520 mm), 859 subjects remain (right- > left-handed individuals: 742, left- > right-handed individuals:  
521 117). Subjects' ages ranged from 8-23 yrs and measures of handedness were based on self-  
522 reports of dominant hand to complete another finger tapping task in the dataset (data not used  
523 in our analyses).

### 524 Preprocessing and generating connectomes

525 Both the HBN and PNC datasets were analyzed with identical processing pipelines. Structural  
526 scans were first skull stripped using an optimized version of the FMRIB's Software Library  
527 (FSL)<sup>69</sup> pipeline<sup>70</sup>. Functional images were motion corrected using SPM12. All further analyses  
528 were performed using BioImage Suite<sup>71</sup> and included linear and nonlinear registration to the  
529 MNI template, unless otherwise specified. Several covariates of no interest were regressed from  
530 the data including linear and quadratic drifts, mean cerebral-spinal-fluid (CSF) signal, mean  
531 white-matter signal, and mean gray matter signal. For additional control of possible motion-  
532 related confounds, a 24-parameter motion model (including six rigid-body motion parameters,  
533 six temporal derivatives, and these terms squared) was regressed from the data. The data were  
534 temporally smoothed with a Gaussian filter (approximate cutoff frequency=0.12 Hz).

535

536 Nodes were defined using the Shen 268-node brain atlas<sup>72</sup>, which includes the cortex,  
537 subcortex, and cerebellum as described in prior CPM work. The atlas was warped from MNI  
538 space into single-subject space via a series of linear and non-linear transformations. Resting  
539 state connectivity was calculated on the basis of the 'raw' task time courses<sup>73</sup>, which

540 emphasizes individual differences in connectivity<sup>43</sup>. This involved computation of the mean time  
541 courses for each of the 268 nodes (i.e., averaging the time courses of all constituent voxels).  
542 Node-by-node pairwise correlations were computed, and Pearson correlation coefficients were  
543 Fisher z-transformed to yield symmetric 268x268 connectivity matrices, in which each element  
544 of the matrix represents the connectivity strength between two individual nodes (i.e., 'edge').

#### 545 Defining Networks of Interest

546 Based on previous literature on differences in handedness<sup>6,8,27-32,49,74</sup>, we defined three  
547 networks of interest: motor, somatosensory, and language using the Brodmann Areas that were  
548 reported for each publication (Table 1). Connectomes were partitioned into matrices that only  
549 contained edges that stem from a node of interest or edges between nodes of interest.  
550 Differences between the left- > right-handed and right- > left-handed groups were estimated  
551 using Network-Based Statistics<sup>17</sup> (component-determining threshold  $z=1.96$ , 2-tailed,  $K=5000$   
552 permutations) for each network separately.

553  
554 Initial analyses conducted on the HBN utilized raw EHQ scores to identify differences between  
555 the left- > right-handed and right- > left-handed groups (Fig. 1), whereas analyses done purely  
556 on the PNC relied on 0/1 self-reported measures of handedness to replicate the same analyses  
557 (Fig. S3).

#### 558 Generalization to the PNC

559 The significance of the overlap between the networks of interest and the whole brain between  
560 the HBN and PNC was determined with the hypergeometric cumulative density function<sup>37</sup>, which  
561 returns the probability of drawing up to  $x$  of  $K$  possible items in  $n$  drawings without replacement  
562 from an  $M$ -item population. This was implemented in Matlab as:  $p=1-hygecdf(x, M, K, n)$ , where  
563  $x$  equals the number of overlapping edges,  $K$  equals the number of connections in the HBN  
564 network of interest,  $n$  equals the number of connections in the PNC network of interest, and  $M$   
565 equals the total number of edges in the matrix (35,778). Percent overlap for the barplots (Figs.  
566 S5 and S9) were calculated as:  $\text{number of overlapping edges}/(\text{HBN significant edges} + \text{PNC}$   
567  $\text{significant edges} - \text{overlapping edges})$ .

#### 568 Combined analyses: HBN + PNC

569 For all analyses where we combined data from the HBN and PNC, we addressed  
570 incongruencies in handedness measures by binarizing EHQ scores such that subjects who  
571 scored below 0 were considered primarily left-handed and above 0 were considered primarily  
572 right-handed. No subject had an EHQ score of exactly 0. Networks of interest analyses  
573 conducted on thresholded HBN EHQ scores at 0 (Fig. S4) exhibited similar patterns of  
574 connectivity both in the brain and circle plots as analyses conducted on raw EHQ scores (Fig.  
575 1).  
576

577 Whole brain functional connectivity differences between left- and right-handed individuals were  
578 estimated using the Network-Based Statistic<sup>17</sup> (component size statistic; component-  
579 determining threshold  $z = 1.96$ , 2-tailed,  $K=5000$  permutations) for each network separately.

580  
581 Due to the large number of edges identified as significant in our whole-brain analyses, we  
582 thresholded our visualizations for the brain and circle plots (Fig. 2A) to degree threshold 50,  
583 brain plots with varying thresholds are shown in SI (Fig. S6). The remainder of our whole-brain  
584 analyses showing the number of significant edges in each anatomical region is based on the full  
585 connectome without thresholds.

586  
587 Similarly, our between and within-hemisphere brain and circle plots (Fig. 4) were thresholded at  
588 degree threshold 25 to demonstrate patterns of connectivity. Visualizations with varying  
589 thresholds are shown in SI (Fig. S10). All quantifications are based on subsetting connectomes  
590 to include only between or within-hemisphere edges without thresholds.

591  
592 Finally, our analyses on the cerebellum brain and circle plots (Fig. 5) show the full set of  
593 significant edges without thresholds to demonstrate patterns of connectivity. All quantifications  
594 are based on subsetting connectomes to include edges between and within the cerebellar  
595 nodes.

#### 596 Effect Size Comparisons

597 In comparing effect sizes between sex and handedness (Fig. 3), effect sizes were calculated for  
598 each edge in a 268x268 connectome across all subjects in both datasets for sex and for  
599 handedness.

#### 600 Controlling for confounding factors in datasets

601 Because we used developmental datasets with some clinical diagnoses to study a normative  
602 trait. We conducted additional analyses using NBS partial correlations to control for sex (Tables  
603 S1, S2) and age (Tables S3, S4) in both the HBN and the PNC to demonstrate the same  
604 significant edges were identified between the left- > right-handed and right- > left-handed  
605 groups while controlling for these differences. Results were split up into two tables when  
606 controlling for sex and age to demonstrate overlaps when analyses were conducted identically  
607 to results section of the paper (sex: Table S1, age: Table S3) and to show results still hold up  
608 when we run NBS on the two datasets, HBN and PNC, for whole brain and cerebellum (sex:  
609 Table S2, age: Table S4) separately. We also controlled for scan site (Table S5) and clinical  
610 diagnoses (Table S6) in the HBN since this sample was collected from many different scan sites  
611 and the population was biased towards clinical diagnoses (794/905 subjects had at least one  
612 clinical diagnosis). Pearson correlations were calculated between matrices of significant edges  
613 identified by NBS alone and NBS correlation controlling for each factor. Unlike our  
614 generalizations from HBN to the PNC, we opted to use correlations as opposed to  
615 hypergeometric cumulative density function (as previously used to show generalization across  
616 datasets) because samples were not independent of each other.

617 **References**

- 618 1. Faurie, C. & Raymond, M. Handedness frequency over more than ten thousand years.  
619 *Proc. Biol. Sci.* **271 Suppl 3**, S43–5 (2004).
- 620 2. Corballis, M. C. From mouth to hand: gesture, speech, and the evolution of right-  
621 handedness. *Behav. Brain Sci.* **26**, 199–208; discussion 208–60 (2003).
- 622 3. Ocklenburg, S., Beste, C., Arning, L., Peterburs, J. & Güntürkün, O. The ontogenesis of  
623 language lateralization and its relation to handedness. *Neurosci. Biobehav. Rev.* **43**, 191–  
624 198 (2014).
- 625 4. Knecht, S. *et al.* Language lateralization in healthy right-handers. *Brain* **123 ( Pt 1)**, 74–81  
626 (2000).
- 627 5. Jang, H., Lee, J. Y., Lee, K. I. & Park, K. M. Are there differences in brain morphology  
628 according to handedness? *Brain Behav.* **7**, e00730 (2017).
- 629 6. Jung, P., Baumgärtner, U., Magerl, W. & Treede, R.-D. Hemispheric asymmetry of hand  
630 representation in human primary somatosensory cortex and handedness. *Clin.*  
631 *Neurophysiol.* **119**, 2579–2586 (2008).
- 632 7. Luders, E. *et al.* When more is less: Associations between corpus callosum size and  
633 handedness lateralization. *NeuroImage* vol. 52 43–49 (2010).
- 634 8. Jörgens, S., Kleiser, R., Indefrey, P. & Seitz, R. J. Handedness and functional MRI-  
635 activation patterns in sentence processing. *Neuroreport* **18**, 1339–1343 (2007).
- 636 9. Grabowska, A. *et al.* Switching handedness: fMRI study of hand motor control in right-  
637 handers, left-handers and converted left-handers. *Acta Neurobiol. Exp.* **72**, 439–451  
638 (2012).
- 639 10. Nenert, R. *et al.* Age-related language lateralization assessed by fMRI: The effects of sex  
640 and handedness. *Brain Res.* **1674**, 20–35 (2017).
- 641 11. Kertesz, A., Polk, M., Black, S. E. & Howell, J. Sex, handedness, and the morphometry of  
642 cerebral asymmetries on magnetic resonance imaging. *Brain Res.* **530**, 40–48 (1990).



- 643 12. Margiotoudi, K. *et al.* Handedness in monkeys reflects hemispheric specialization within the  
644 central sulcus. An in vivo MRI study in right- and left-handed olive baboons. *Cortex* **118**,  
645 203–211 (2019).
- 646 13. Rosch, R. E., Cowell, P. E. & Gurd, J. M. Cerebellar Asymmetry and Cortical Connectivity  
647 in Monozygotic Twins with Discordant Handedness. *Cerebellum* **17**, 191–203 (2018).
- 648 14. Kirsch, V. *et al.* Handedness-dependent functional organizational patterns within the  
649 bilateral vestibular cortical network revealed by fMRI connectivity based parcellation.  
650 *NeuroImage* vol. 178 224–237 (2018).
- 651 15. Pool, E.-M., Rehme, A. K., Eickhoff, S. B., Fink, G. R. & Grefkes, C. Functional resting-  
652 state connectivity of the human motor network: differences between right- and left-handers.  
653 *Neuroimage* **109**, 298–306 (2015).
- 654 16. Li, M. *et al.* Increased cortical thickness and altered functional connectivity of the right  
655 superior temporal gyrus in left-handers. *Neuropsychologia* **67**, 27–34 (2015).
- 656 17. Zalesky, A., Fornito, A. & Bullmore, E. T. Network-based statistic: Identifying differences in  
657 brain networks. *NeuroImage* vol. 53 1197–1207 (2010).
- 658 18. Hatta, T. Handedness and the Brain: A Review of Brain-imaging Techniques. *Magnetic*  
659 *Resonance in Medical Sciences* vol. 6 99–112 (2007).
- 660 19. Szaflarski, J. P. *et al.* Left-handedness and language lateralization in children. *Brain Res.*  
661 **1433**, 85–97 (2012).
- 662 20. Wiberg, A. *et al.* Handedness, language areas and neuropsychiatric diseases: insights from  
663 brain imaging and genetics. *Brain* **142**, 2938–2947 (2019).
- 664 21. Shen, X. *et al.* Using connectome-based predictive modeling to predict individual behavior  
665 from brain connectivity. *Nat. Protoc.* **12**, 506–518 (2017).
- 666 22. Nelson, E. L., Campbell, J. M. & Michel, G. F. Early handedness in infancy predicts  
667 language ability in toddlers. *Dev. Psychol.* **50**, 809–814 (2014).
- 668 23. Alexander, L. M. *et al.* An open resource for transdiagnostic research in pediatric mental

- 669 health and learning disorders. *Sci Data* **4**, 170181 (2017).
- 670 24. Satterthwaite, T. D. *et al.* The Philadelphia Neurodevelopmental Cohort: A publicly  
671 available resource for the study of normal and abnormal brain development in youth.  
672 *NeuroImage* vol. 124 1115–1119 (2016).
- 673 25. Hirnstein, M. & Hugdahl, K. Excess of non-right-handedness in schizophrenia: meta-  
674 analysis of gender effects and potential biases in handedness assessment. *Br. J.*  
675 *Psychiatry* **205**, 260–267 (2014).
- 676 26. Satterthwaite, T. D. *et al.* Neuroimaging of the Philadelphia Neurodevelopmental Cohort.  
677 *NeuroImage* vol. 86 544–553 (2014).
- 678 27. Longcamp, M., Anton, J.-L., Roth, M. & Velay, J.-L. Premotor activations in response to  
679 visually presented single letters depend on the hand used to write: a study on left-handers.  
680 *Neuropsychologia* vol. 43 1801–1809 (2005).
- 681 28. Amunts, K., Jäncke, L., Mohlberg, H., Steinmetz, H. & Zilles, K. Interhemispheric  
682 asymmetry of the human motor cortex related to handedness and gender.  
683 *Neuropsychologia* **38**, 304–312 (2000).
- 684 29. Gorrie, C. A., Waite, P. M. E. & Rogers, L. J. Correlations between hand preference and  
685 cortical thickness in the secondary somatosensory (SII) cortex of the common marmoset,  
686 *Callithrix jacchus*. *Behav. Neurosci.* **122**, 1343–1351 (2008).
- 687 30. Meguerditchian, A., Gardner, M. J., Schapiro, S. J. & Hopkins, W. D. The sound of one-  
688 hand clapping: handedness and perisylvian neural correlates of a communicative gesture in  
689 chimpanzees. *Proc. Biol. Sci.* **279**, 1959–1966 (2012).
- 690 31. Falk, D. Language, Handedness, and Primate Brains: Did the Australopithecines Sign?  
691 *American Anthropologist* vol. 82 72–78 (1980).
- 692 32. Foundas, A. L., Eure, K. F., Luevano, L. F. & Weinberger, D. R. MRI asymmetries of  
693 Broca's area: the pars triangularis and pars opercularis. *Brain Lang.* **64**, 282–296 (1998).
- 694 33. Gao, J. H. *et al.* Cerebellum implicated in sensory acquisition and discrimination rather than

- 695 motor control. *Science* **272**, 545–547 (1996).
- 696 34. Cui, Z. *et al.* Individual Variation in Functional Topography of Association Networks in  
697 Youth. *Neuron* **106**, 340–353.e8 (2020).
- 698 35. Takanashi, M. *et al.* A functional MRI study of somatotopic representation of  
699 somatosensory stimulation in the cerebellum. *Neuroradiology* **45**, 149–152 (2003).
- 700 36. Duffau, H., Leroy, M. & Gatignol, P. Cortico-subcortical organization of language networks  
701 in the right hemisphere: an electrostimulation study in left-handers. *Neuropsychologia* **46**,  
702 3197–3209 (2008).
- 703 37. Rosenberg, M. D. *et al.* Methylphenidate Modulates Functional Network Connectivity to  
704 Enhance Attention. *J. Neurosci.* **36**, 9547–9557 (2016).
- 705 38. Hécaen, H. & Sauguet, J. Cerebral dominance in left-handed subjects. *Cortex* **7**, 19–48  
706 (1971).
- 707 39. Noble, S., Scheinost, D. & Todd Constable, R. Cluster failure or power failure? Evaluating  
708 sensitivity in cluster-level inference. *NeuroImage* vol. 209 116468 (2020).
- 709 40. Scott Marek, Brenden Tervo-Clemmens, Finnegan J. Calabro, David F. Montez, Benjamin  
710 P. Kay, Alexander S. Hatoum, Meghan Rose Donohue, William Foran, Ryland L. Miller, Eric  
711 Feczko, Oscar Miranda-Dominguez, Alice M. Graham, Eric A. Earl, Anders J. Perrone,  
712 Michaela Cordova, Olivia Doyle, Lucille A. Moore, Greg Conan, Johnny Uriarte, Kathy  
713 Snider, Angela Tam, Jianzhong Chen, Dillan J. Newbold, Annie Zheng, Nicole A. Seider,  
714 Andrew N. Van, Timothy O. Laumann, Wesley K. Thompson, Deanna J. Greene, Steven E.  
715 Petersen, Thomas E. Nichols, B.T. Thomas Yeo, Deanna M. Barch, Hugh Garavan, Beatriz  
716 Luna, Damien A. Fair, Nico U.F. Dosenbach. Towards Reproducible Brain-Wide  
717 Association Studies. *bioRxiv* (2020).
- 718 41. Noble, S. *et al.* Influences on the Test–Retest Reliability of Functional Connectivity MRI and  
719 its Relationship with Behavioral Utility. *Cerebral Cortex* vol. 27 5415–5429 (2017).
- 720 42. Finn, E. S. *et al.* Functional connectome fingerprinting: identifying individuals using patterns

- 721 of brain connectivity. *Nat. Neurosci.* **18**, 1664–1671 (2015).
- 722 43. Anticevic, A. *et al.* Global Resting-State Functional Magnetic Resonance Imaging Analysis  
723 Identifies Frontal Cortex, Striatal, and Cerebellar Dysconnectivity in Obsessive-Compulsive  
724 Disorder. *Biol. Psychiatry* **75**, 595–605 (2014).
- 725 44. Isaacs, K. L., Barr, W. B., Nelson, P. K. & Devinsky, O. Degree of handedness and cerebral  
726 dominance. *Neurology* vol. 66 1855–1858 (2006).
- 727 45. Kavaklioglu, T. *et al.* Structural asymmetries of the human cerebellum in relation to cerebral  
728 cortical asymmetries and handedness. *Brain Struct. Funct.* **222**, 1611–1623 (2017).
- 729 46. Jung, P. *et al.* Asymmetry in the human primary somatosensory cortex and handedness.  
730 *NeuroImage* vol. 19 913–923 (2003).
- 731 47. Zhiqiang Sha, Antonietta Pepe, Dick Schijven, Amaia Carrion Castillo, James M. Roe,  
732 René Westerhausen, Marc Joliot, Simon E. Fisher, Fabrice Crivello, Clyde Francks. Left-  
733 handedness and its genetic influences are associated with structural asymmetries mapped  
734 across the cerebral cortex in 31,864 individuals. *bioRxiv* (2021).
- 735 48. Chapman, L. J. & Chapman, J. P. The measurement of handedness. *Brain Cogn.* **6**, 175–  
736 183 (1987).
- 737 49. Pool, E.-M., Rehme, A. K., Fink, G. R., Eickhoff, S. B. & Grefkes, C. Handedness and  
738 effective connectivity of the motor system. *Neuroimage* **99**, 451–460 (2014).
- 739 50. Amunts, K. *et al.* Asymmetry in the Human Motor Cortex and Handedness. *NeuroImage*  
740 vol. 4 216–222 (1996).
- 741 51. Dassonville, P., Zhu, X. H., Uurbil, K., Kim, S. G. & Ashe, J. Functional activation in motor  
742 cortex reflects the direction and the degree of handedness. *Proc. Natl. Acad. Sci. U. S. A.*  
743 **94**, 14015–14018 (1997).
- 744 52. Kim, S. *et al.* Functional magnetic resonance imaging of motor cortex: hemispheric  
745 asymmetry and handedness. *Science* vol. 261 615–617 (1993).
- 746 53. Paulin, M. G. The Role of the Cerebellum in Motor Control and Perception. *Brain, Behavior*

- 747           *and Evolution* vol. 41 39–50 (1993).
- 748   54. Ebner, T. J. & Pasalar, S. Cerebellum Predicts the Future Motor State. *The Cerebellum* vol.  
749       7 583–588 (2008).
- 750   55. Buckner, R. L. The cerebellum and cognitive function: 25 years of insight from anatomy and  
751       neuroimaging. *Neuron* **80**, 807–815 (2013).
- 752   56. McClatchy, D. B., Liao, L., Park, S. K., Venable, J. D. & Yates, J. R. Quantification of the  
753       synaptosomal proteome of the rat cerebellum during post-natal development. *Genome*  
754       *Research* vol. 17 1378–1388 (2007).
- 755   57. Helpman, L. *et al.* Sex Differences in Trauma-Related Psychopathology: a Critical Review  
756       of Neuroimaging Literature (2014–2017). *Current Psychiatry Reports* vol. 19 (2017).
- 757   58. Gaillard, A., Fehring, D. J. & Rossell, S. L. Sex differences in executive control: A  
758       systematic review of functional neuroimaging studies. *Eur. J. Neurosci.* **53**, 2592–2611  
759       (2021).
- 760   59. Rippon, G., Jordan-Young, R., Kaiser, A. & Fine, C. Recommendations for sex/gender  
761       neuroimaging research: key principles and implications for research design, analysis, and  
762       interpretation. *Front. Hum. Neurosci.* **8**, 650 (2014).
- 763   60. Jack, A. & A Pelphrey, K. Annual Research Review: Understudied populations within the  
764       autism spectrum - current trends and future directions in neuroimaging research. *J. Child*  
765       *Psychol. Psychiatry* **58**, 411–435 (2017).
- 766   61. Vargha-Khadem, F., O’Gorman, A. M. & Watters, G. V. Aphasia and handedness in relation  
767       to hemispheric side, age at injury and severity of cerebral lesion during childhood. *Brain*  
768       **108 ( Pt 3)**, 677–696 (1985).
- 769   62. Tomasi, D., Wang, R., Wang, G.-J. & Volkow, N. D. Functional connectivity and brain  
770       activation: a synergistic approach. *Cereb. Cortex* **24**, 2619–2629 (2014).
- 771   63. Knecht, S. Handedness and hemispheric language dominance in healthy humans. *Brain*  
772       vol. 123 2512–2518 (2000).

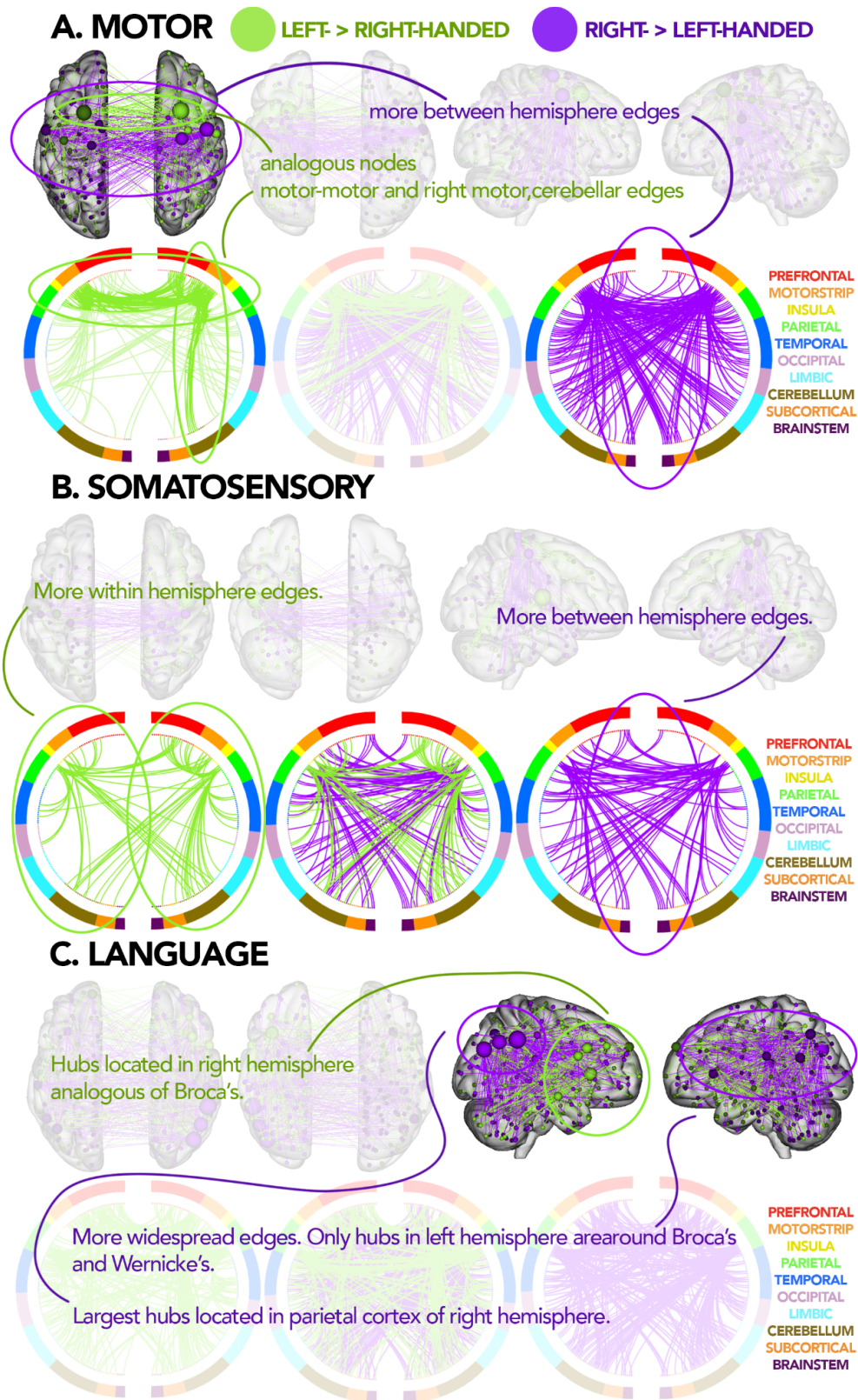
- 773 64. Ardila, A. *et al.* Effects of cultural background and education on handedness.  
774 *Neuropsychologia* **27**, 893–897 (1989).
- 775 65. Hepper, P. G., Wells, D. L. & Lynch, C. Prenatal thumb sucking is related to postnatal  
776 handedness. *Neuropsychologia* vol. 43 313–315 (2005).
- 777 66. Edlin, J. M. *et al.* On the use (and misuse?) of the Edinburgh Handedness Inventory. *Brain*  
778 *Cogn.* **94**, 44–51 (2015).
- 779 67. Levy, J. & Reid, M. Variations in cerebral organization as a function of handedness, hand  
780 posture in writing, and sex. *J. Exp. Psychol. Gen.* **107**, 119–144 (1978).
- 781 68. Papadatou-Pastou, M., Martin, M., Munafò, M. R. & Jones, G. V. Sex differences in left-  
782 handedness: a meta-analysis of 144 studies. *Psychol. Bull.* **134**, 677–699 (2008).
- 783 69. Smith, S. M. *et al.* Advances in functional and structural MR image analysis and  
784 implementation as FSL. *Neuroimage* **23 Suppl 1**, S208–19 (2004).
- 785 70. Lutkenhoff, E. S. *et al.* Optimized brain extraction for pathological brains (optiBET). *PLoS*  
786 *One* **9**, e115551 (2014).
- 787 71. Joshi, A. *et al.* Unified framework for development, deployment and robust testing of  
788 neuroimaging algorithms. *Neuroinformatics* **9**, 69–84 (2011).
- 789 72. Shen, X., Tokoglu, F., Papademetris, X. & Constable, R. T. Groupwise whole-brain  
790 parcellation from resting-state fMRI data for network node identification. *NeuroImage* vol.  
791 82 403–415 (2013).
- 792 73. Greene, A. S., Gao, S., Noble, S., Scheinost, D. & Constable, R. T. How Tasks Change  
793 Whole-Brain Functional Organization to Reveal Brain-Phenotype Relationships. *Cell Rep.*  
794 **32**, 108066 (2020).
- 795 74. Joliot, M., Tzourio-Mazoyer, N. & Mazoyer, B. Intra-hemispheric intrinsic connectivity  
796 asymmetry and its relationships with handedness and language Lateralization.  
797 *Neuropsychologia* **93**, 437–447 (2016).

## 798 **Supplementary Results**

### 799 *Generalization of whole-brain results between the HBN and PNC*

800 To verify that results generalized across datasets at the level of the whole brain, rather than just  
801 within the networks of interest, we performed cluster-based inference on the entire connectome  
802 for the HBN and PNC separately, then proceeded to look at the number of overlapping edges, in  
803 the same manner as above. Generalization between the two datasets revealed significance  
804 across the whole brain and across all data-driven functional networks, analogous to functional  
805 networks of interest (Fig. S9). Across all canonical brain networks<sup>41,42</sup>, the number of  
806 overlapping edges far exceeds the minimum level required for significance, with t  
807 he exception of the salience network in the right- > left-handed group. At the whole brain level,  
808 slightly greater than 3% of the total number of edges overlap between the HBN and PNC  
809 results. Given that a connectome has 35,778 unique edges, it is exceedingly rare to choose a  
810 single edge out of two random draws from all edges, let alone the 91 overlapping edges we  
811 observe. Together with the network of interest results, these results repeatedly demonstrate that  
812 edges observed to significantly differ between the left- > right-handed and right- > left-handed  
813 groups are highly generalizable across datasets, despite differences in study design including,  
814 handedness measure and scanner/scan sites.Between and within hemispheres  
815 A common observation from our whole-brain analyses was that the left- > right-handed and  
816 right- > left-handed groups differed in the patterns of edges forming between and within-  
817 hemispheres. Thus, we performed NBS on connectomes subsetted for within- and between  
818 networks separately.

819 **Supplementary Figures**

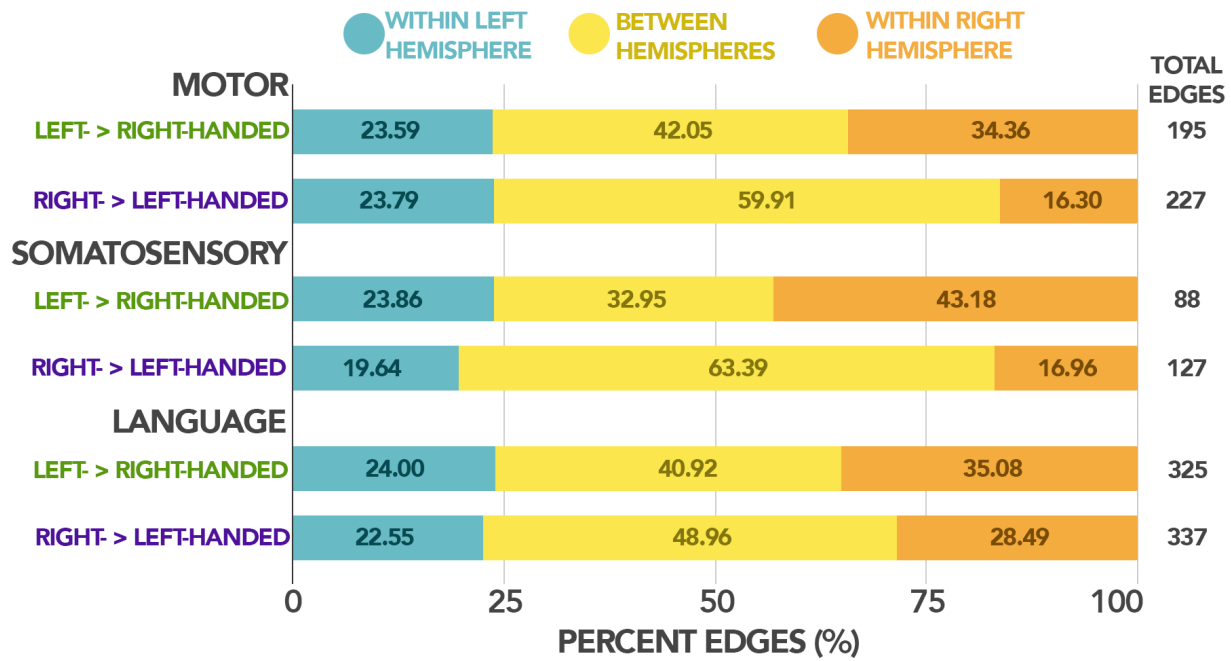


820  
821

**Fig. S1:** Summarization of results from Fig. 1 showing only patterns of interest.



822

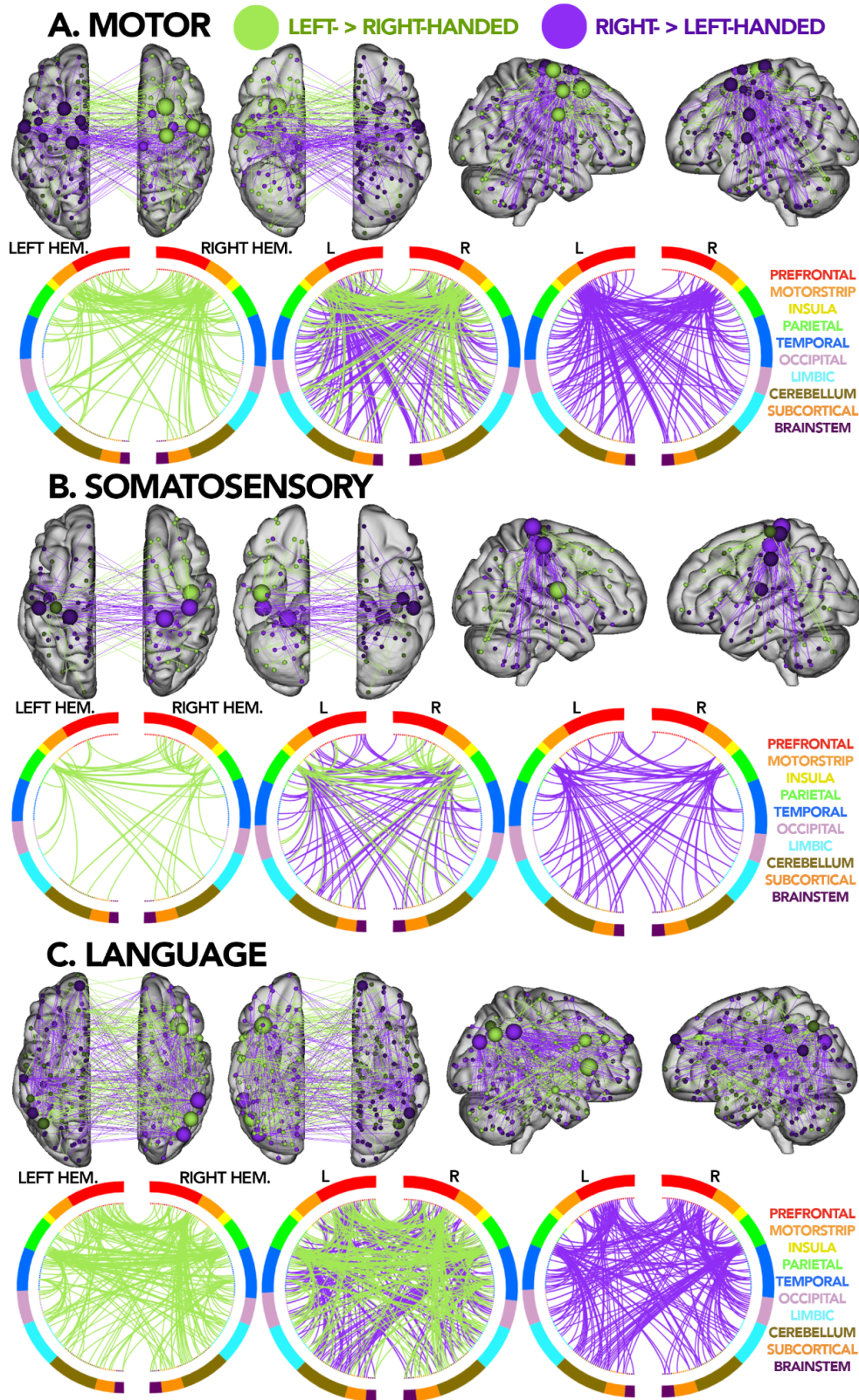


823

824

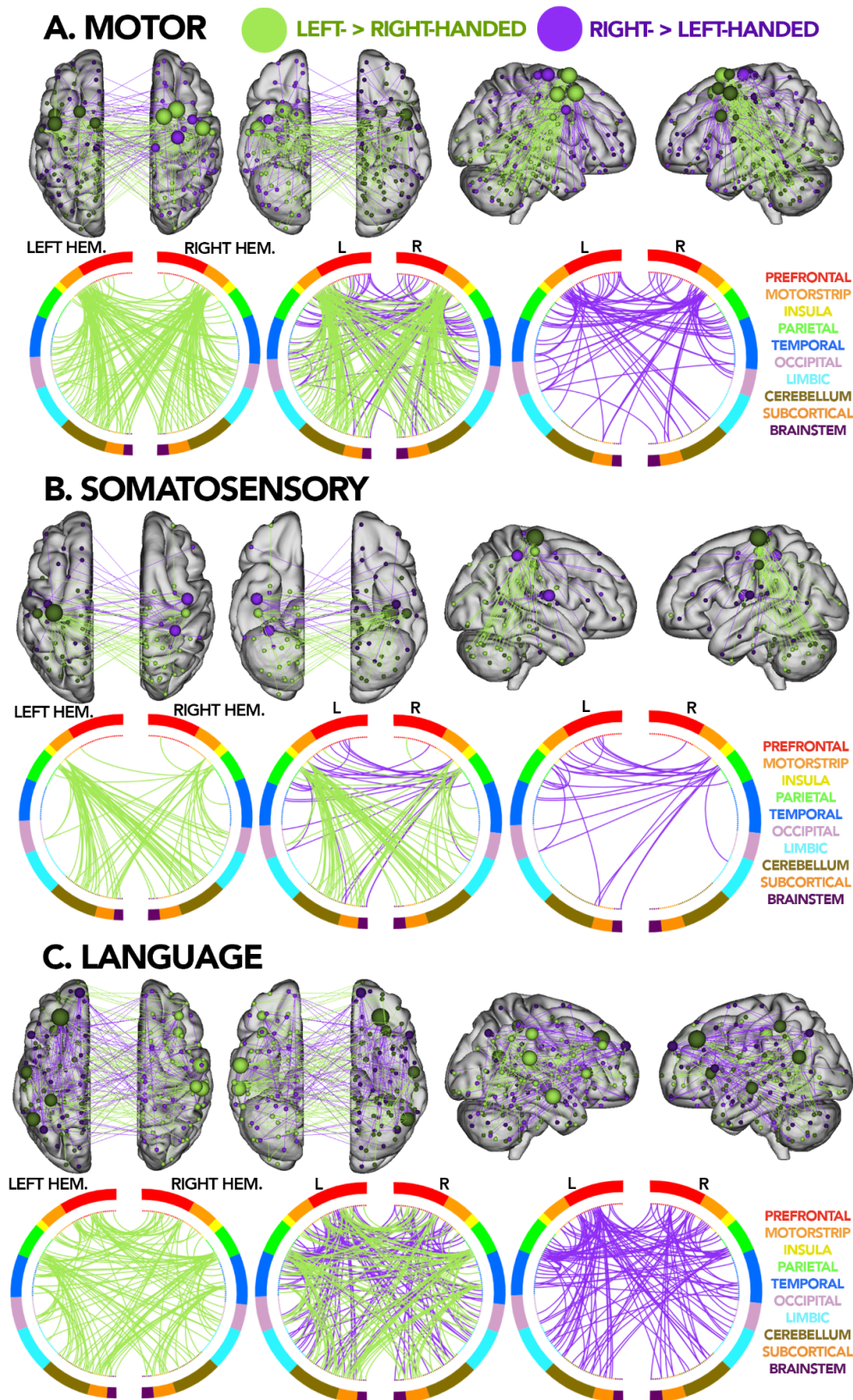
825

**Fig. S2:** Percent of edges in each network of interest: motor, somatosensory, and language, split by left- > right-handed group and right- > left-handed group connecting within left/right hemispheres or between-hemispheres.



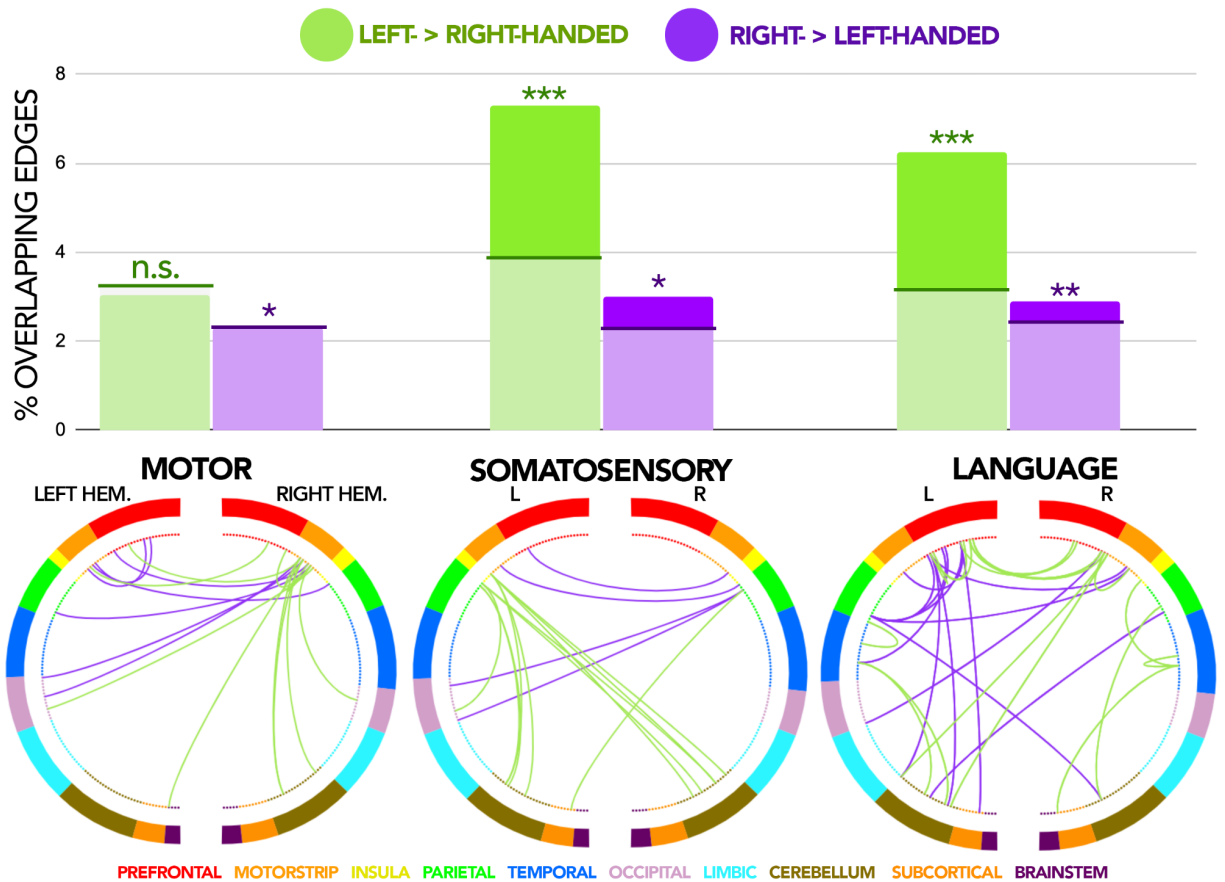
826  
827  
828

**Fig. S3:** Replication of same networks of interest conducted in Fig. 1 but with raw EHQ scores converted to 0/1, thresholded at 0. EHQ scores < 0 = left- > right-handed group, EHQ scores > 0 = right- > left-handed group.



829  
830  
831

**Fig. S4:** Replication of same networks of interest conducted in Fig. 1 but with data from the PNC. Behavioral scores were binarized for left- > right-handed and right- > left-handed participants.



832

833

834

835

836

837

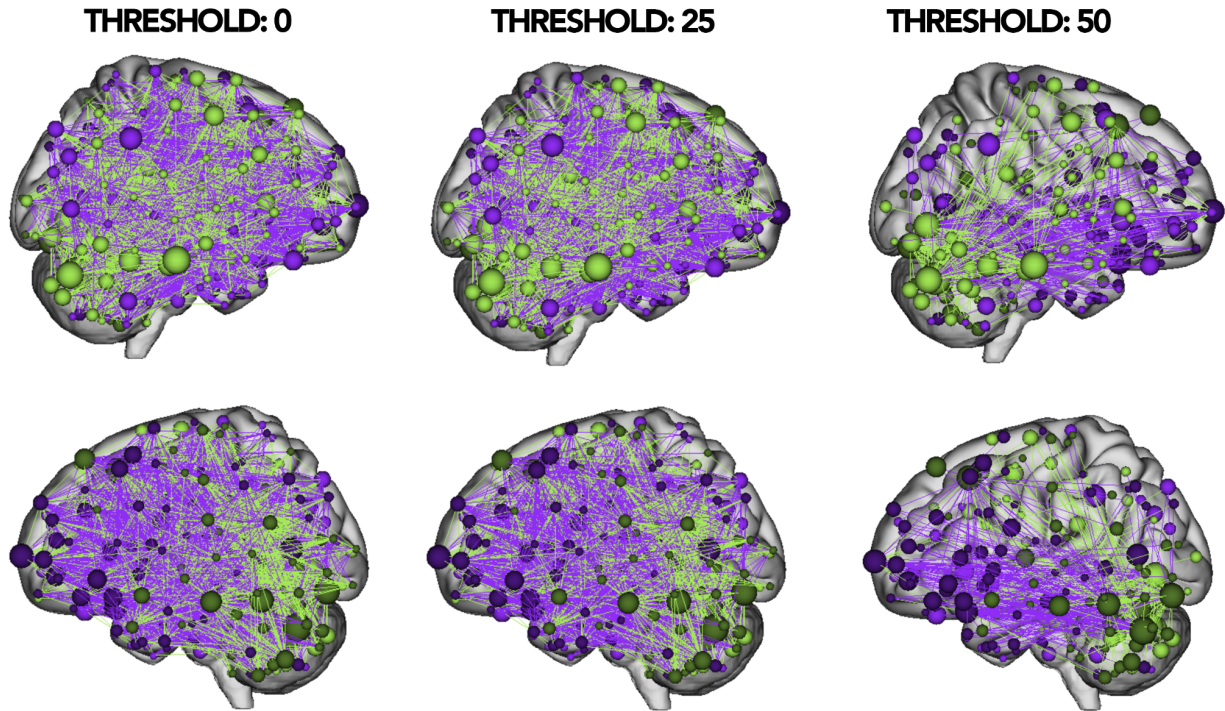
838

839

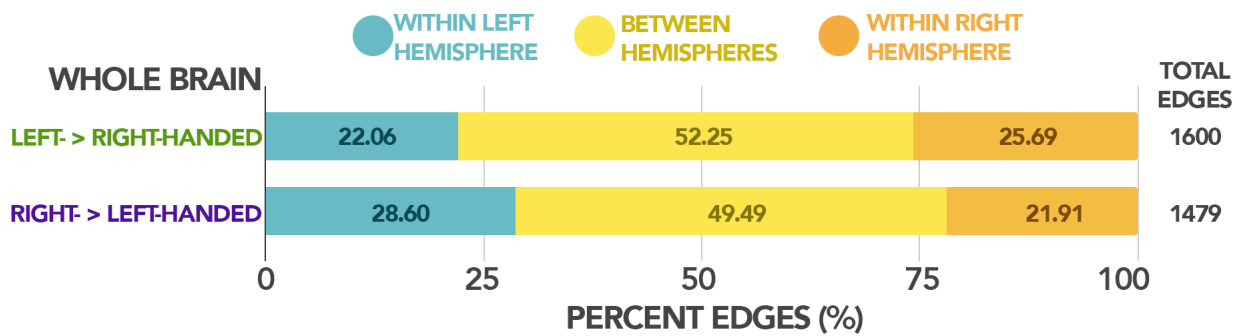
840

**Fig. S5:** Bottom row shows circle plots where the left and right hemispheres are depicted as left and right semi-circles, respectively. Nodes are color-coded by anatomical networks constructed based on the Shen atlas, each line depicts a significant edge identified through NBS. Legend for which anatomical region each color represents is shown in a line above the three circle plots. Each circle plot shows significant edges that are present in both HBN and PNC for each network of interest: motor, somatosensory, and language, respectively. Top row depicts a bar graph of % overlapping edges for each network of interest. Lines and shaded regions in each bar indicate the minimum % of overlapping edges required for significance. \* on top of each bar indicates significance where n.s. indicates not significant, \* indicates  $p \leq 0.05$ , \*\* indicates  $p \leq 0.01$ , and \*\*\* indicates  $p \leq 0.001$ .

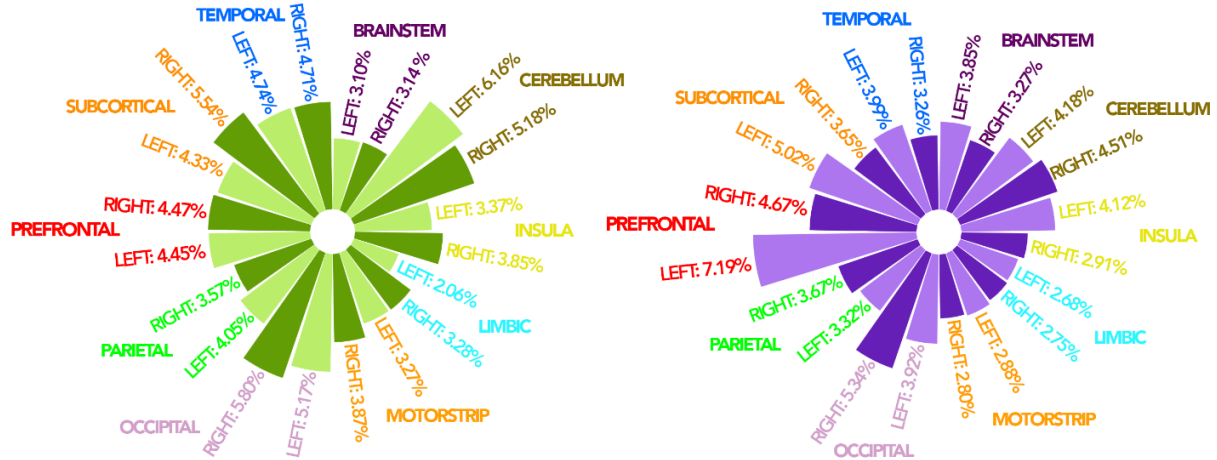
## WHOLE BRAIN



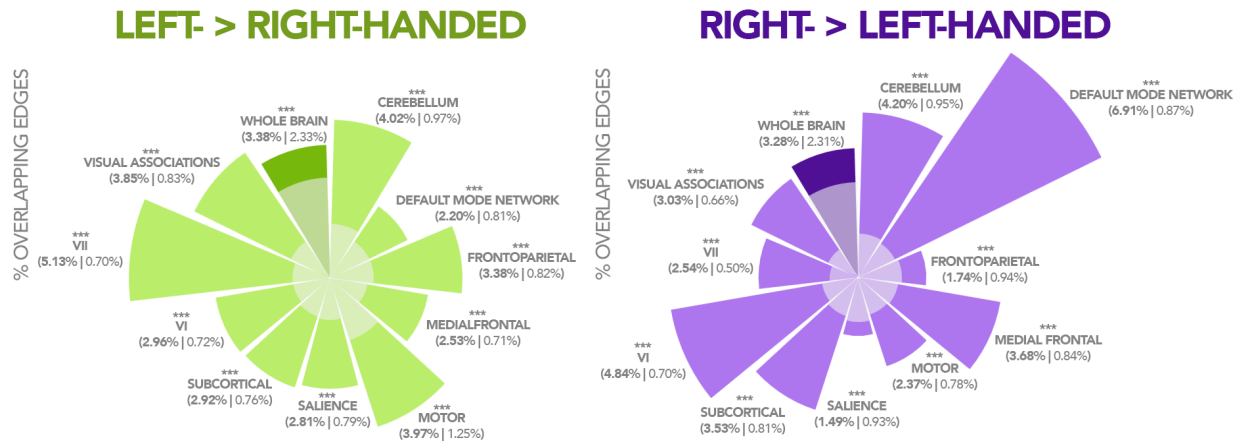
841  
842 **Fig. S6:** Ball-stick brain plots for differences between left-handed individuals and right-handed individuals at the level  
843 of the whole brain for the combined analyses with HBN and PNC thresholded at degree = 0, 25, and 50.  
844



845  
846 **Fig. S7:** Percent of edges for left- > right-handed and right- > left-handed group for edges connecting within left/right  
847 hemispheres or between-hemispheres.  
848



849  
850 **Fig. S8:** Percent of edges that identified as significant in whole brain analysis out of the total number of edges in each  
851 anatomical region, split by left and right hemispheres. Results for left-handed individuals shown in green circular bar  
852 graph on the left and results for right-handed individuals shown in purple circular bar graph on the right. Left  
853 hemispheres shown in lighter colored bars, right hemispheres shown in darker colored bars.  
854



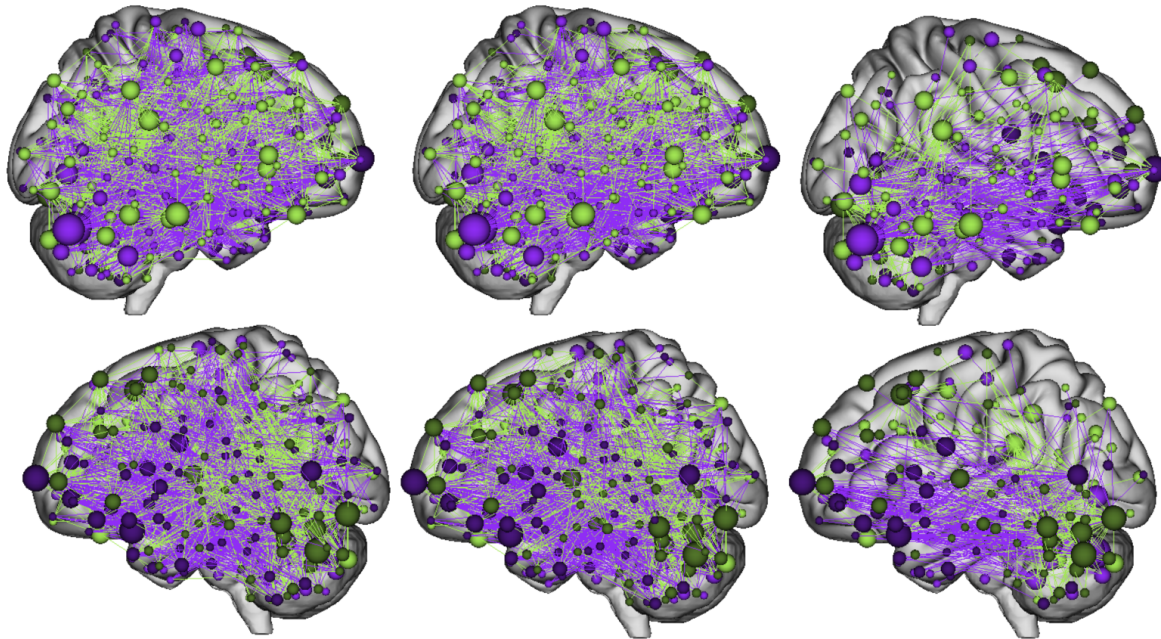
855  
856 **Fig. S9:** Circular bar graphs showing overlapping edges between HBN and PNC by canonical data-driven networks:  
857 Medial Frontal, Frontoparietal, Default Mode Network, Motor, VI, VII, Visual Association, Salience, Subcortical, and  
858 Cerebellum. The whole brain is shown in a darker colored bar for both the left- > right-handed and right- > left-handed  
859 group. Exact percentage of overlapping edges between HBN and PNC shown as the bold value in parentheses; the  
860 second percentage shows the minimum percentage of edges required for results to be significant. The shaded  
861 regions in each circular bar show the minimum percentage of edges required for significance with a p-value below  
862 0.05. \* above each of the labels show significance for each network and the whole brain. \* indicates  $p \leq 0.05$ , \*\*  
863 indicates  $p \leq 0.01$ , and \*\*\* indicates  $p \leq 0.001$

## BETWEEN HEMISPHERES

THRESHOLD: 0

THRESHOLD: 13

THRESHOLD: 25

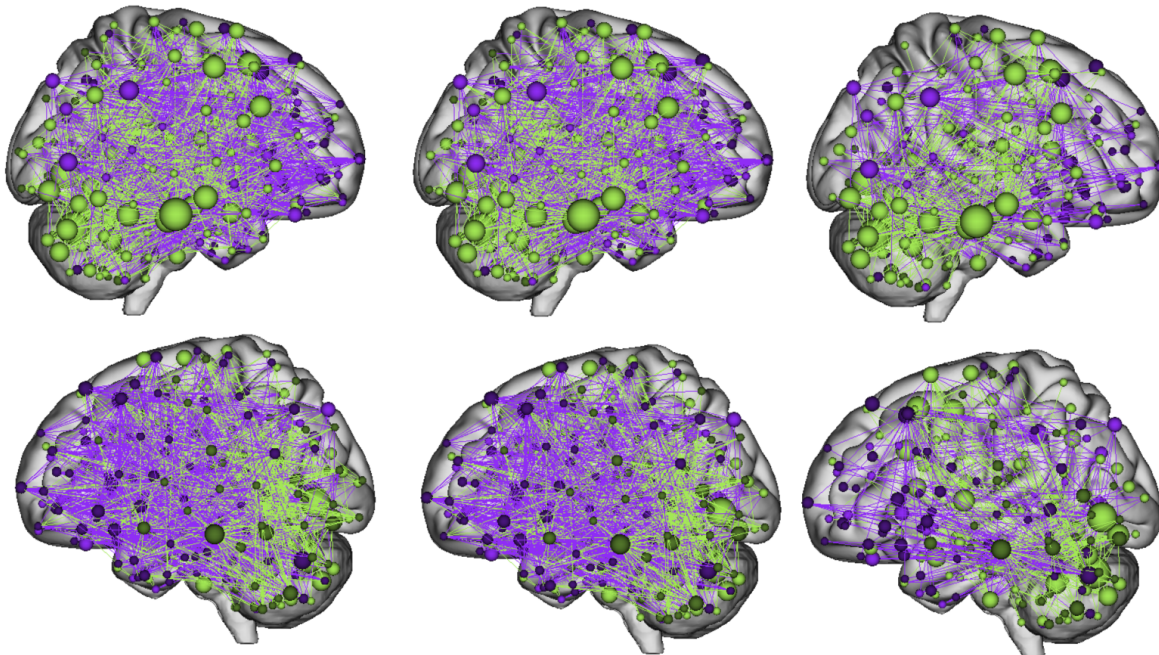


## WITHIN HEMISPHERES

THRESHOLD: 0

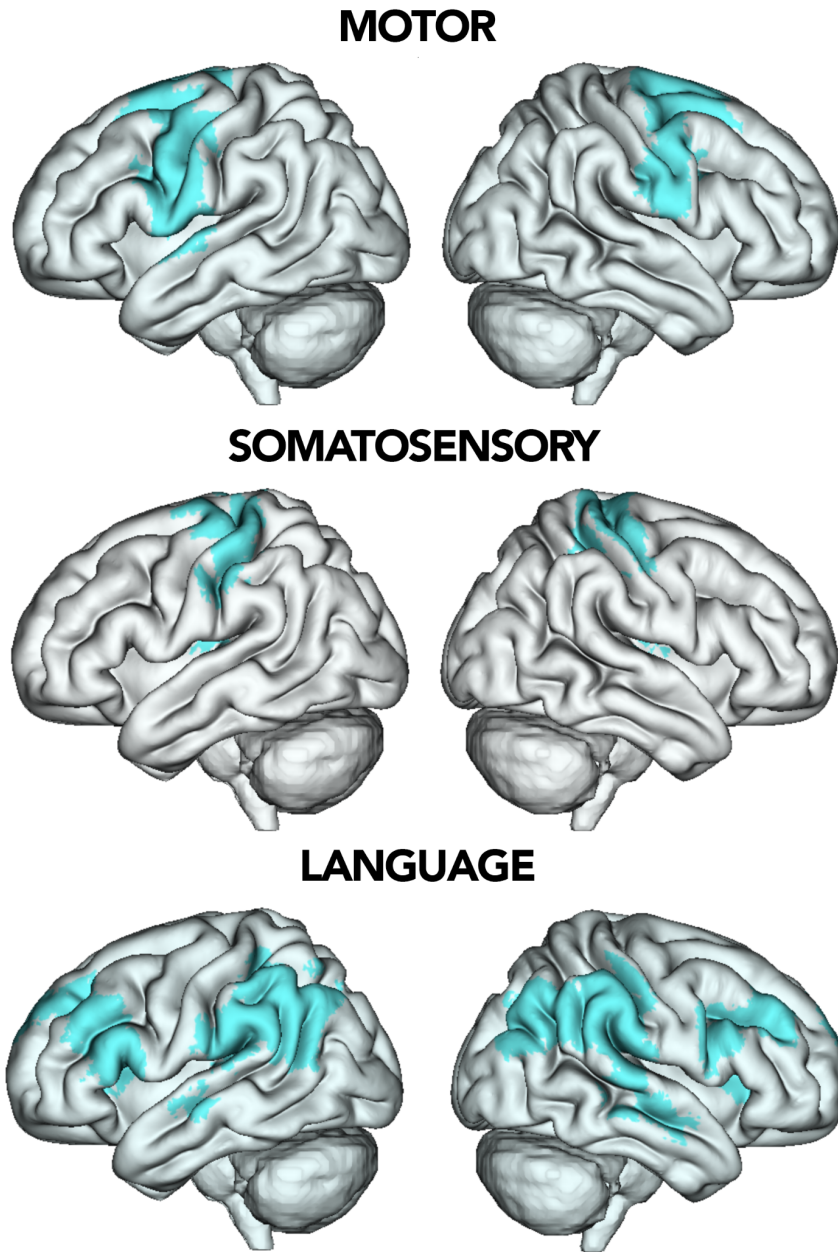
THRESHOLD: 13

THRESHOLD: 25

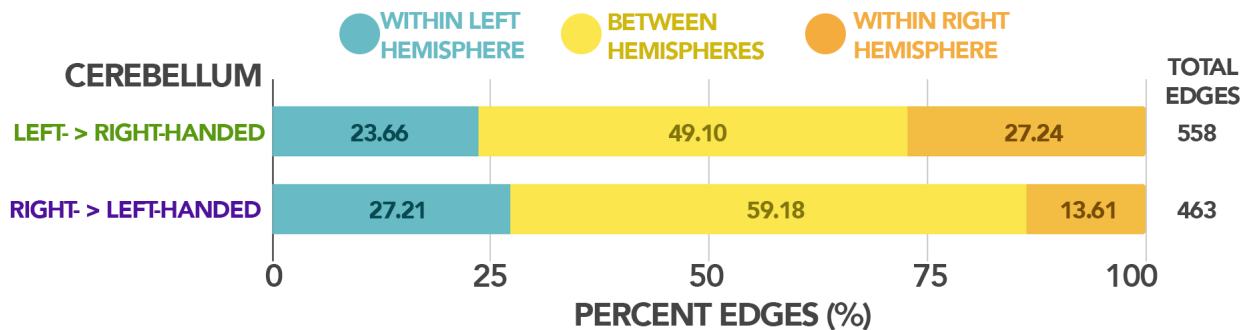


864  
865  
866  
867

**Fig. S10:** Brain plots for differences between left-handed individuals and right-handed individuals between and within-hemispheres for combined analyses with HBN and PNC thresholded at degree = 0, 13, and 25.



868  
869 **Fig. S11:** 3D brain plots showing where nodes for each network of interest are located.  
870



871  
872 **Fig. S12:** Percent of edges in our cerebellum analysis split by left- and right-handed individuals connecting within  
873 left/right hemispheres or between-hemispheres.



874 **Supplementary Tables**

875

	<b>Handedness group</b>	<b>Control for Sex</b>	<b>Handedness only</b>	<b>Overlapping edges</b>	<b>r-val</b>
<b>HBN: Motor</b>	<b>Left &gt; Right</b>	194	195	181	0.9917
	<b>Right &gt; Left</b>	217	227	205	0.9879
<b>HBN: Somatosensory</b>	<b>Left &gt; Right</b>	93	88	85	0.9912
	<b>Right &gt; Left</b>	105	112	100	0.9903
<b>HBN: Language</b>	<b>Left &gt; Right</b>	338	325	315	0.9937
	<b>Right &gt; Left</b>	332	337	324	0.9943
<b>HBN+PNC: Whole Brain</b>	<b>Left &gt; Right</b>	1566	1600	1501	0.9888
	<b>Right &gt; Left</b>	1452	1479	1396	0.9865
<b>HBN+PNC: Cerebellum</b>	<b>Left &gt; Right</b>	529	558	509	0.9938
	<b>Right &gt; Left</b>	439	463	431	0.9940

876 **Table S1:** Replicating all HBN analyses in networks of interest: motor, somatosensory, language, and HBN+PNC  
 877 analyses in whole brain and cerebellum while controlling for sex. Table shows comparison between significant edges  
 878 when controlling for sex and for handedness alone, the overlapping edges between these two analyses and the  
 879 correlation between the two analyses (reported as r values).  
 880

	<b>Handedness group</b>	<b>Control for Sex</b>	<b>Handedness only</b>	<b>Overlapping edges</b>	<b>r-val</b>
<b>HBN: Whole Brain</b>	<b>Left &gt; Right</b>	1385	1925	986	0.8320
	<b>Right &gt; Left</b>	1429	1858	1025	0.7844
<b>HBN: Cerebellum</b>	<b>Left &gt; Right</b>	460	691	354	0.9359
	<b>Right &gt; Left</b>	421	633	328	0.8962
<b>PNC: Whole Brain</b>	<b>Left &gt; Right</b>	1005	1008	967	0.9877
	<b>Right &gt; Left</b>	988	1006	964	0.9912
<b>PNC: Cerebellum</b>	<b>Left &gt; Right</b>	359	359	346	0.9948
	<b>Right &gt; Left</b>	395	404	389	0.9959

881 **Table S2:** Conducting whole brain and cerebellum analyses for HBN and PNC. Comparing significant edges while  
 882 controlling for sex and for handedness alone, the overlapping edges between these two analyses and the correlation  
 883 between the two analyses (reported as r values).  
 884

	Handedness group	Control for Age	Handedness only	Overlapping edges	r-val
<b>HBN: Motor</b>	<b>Left &gt; Right</b>	149	195	147	0.9620
	<b>Right &gt; Left</b>	187	227	179	0.9800
<b>HBN: Somatosensory</b>	<b>Left &gt; Right</b>	62	88	62	0.9660
	<b>Right &gt; Left</b>	91	112	86	0.9748
<b>HBN: Language</b>	<b>Left &gt; Right</b>	252	325	245	0.9809
	<b>Right &gt; Left</b>	269	337	262	0.9710
<b>HBN+PNC: Whole Brain</b>	<b>Left &gt; Right</b>	8382	1600	749	0.9010
	<b>Right &gt; Left</b>	7872	1479	682	0.8982
<b>HBN+PNC: Cerebellum</b>	<b>Left &gt; Right</b>	4014	558	235	0.6406
	<b>Right &gt; Left</b>	3669	463	206	0.5272

885 **Table S3:** Replicating all HBN analyses in networks of interest: motor, somatosensory, language, and HBN+PNC  
 886 analyses in whole brain and cerebellum while controlling for age. Table shows comparison between significant edges  
 887 when controlling for age and for handedness alone, the overlapping edges between these two analyses and the  
 888 correlation between the two analyses (reported as r values).  
 889

	Handedness group	Control for Age	Handedness only	Overlapping edges	r-val
<b>HBN: Whole Brain</b>	<b>Left &gt; Right</b>	1526	1925	1153	0.7941
	<b>Right &gt; Left</b>	1473	1858	1199	0.7104
<b>HBN: Cerebellum</b>	<b>Left &gt; Right</b>	537	691	376	0.9179
	<b>Right &gt; Left</b>	485	633	327	0.8508
<b>PNC: Whole Brain</b>	<b>Left &gt; Right</b>	981	1008	938	0.9800
	<b>Right &gt; Left</b>	953	1006	932	0.9833
<b>PNC: Cerebellum</b>	<b>Left &gt; Right</b>	349	359	336	0.9914
	<b>Right &gt; Left</b>	368	404	358	0.9906

890 **Table S4:** Conducting whole brain and cerebellum analyses for HBN and PNC. Comparing significant edges while  
 891 controlling for age and for handedness alone, the overlapping edges between these two analyses and the correlation  
 892 between the two analyses (reported as r values).  
 893

	Handedness group	Control for Scanning Site	Handedness only	Overlapping edges	r-val
<b>HBN: Motor</b>	Left > Right	195	195	191	0.9975
	Right > Left	225	227	224	0.9989
<b>HBN: Somatosensory</b>	Left > Right	88	88	87	0.9981
	Right > Left	110	112	108	0.9961
<b>HBN: Language</b>	Left > Right	328	325	324	0.9991
	Right > Left	340	337	334	0.9991
<b>HBN: Whole Brain</b>	Left > Right	1936	1925	1902	0.9976
	Right > Left	1858	1858	1830	0.9966
<b>HBN: Cerebellum</b>	Left > Right	695	691	685	0.9992
	Right > Left	636	633	624	0.9985

894 **Table S5:** Replicating all HBN analyses in networks of interest: motor, somatosensory, language, as well as analyses  
 895 in whole brain and cerebellum while controlling for scanning site. Table shows comparison between significant edges  
 896 when controlling for scanning site, the overlapping edges between these two analyses and the correlation between  
 897 the two analyses (reported as r values).  
 898

	Handedness group	Control for Clinical Diagnoses	Handedness only	Overlapping edges	r-val
<b>HBN: Motor</b>	Left > Right	195	195	191	0.9975
	Right > Left	226	227	224	0.9989
<b>HBN: Somatosensory</b>	Left > Right	88	88	87	0.9988
	Right > Left	110	112	108	0.9961
<b>HBN: Language</b>	Left > Right	328	325	324	0.9991
	Right > Left	340	337	336	0.9980
<b>HBN: Whole Brain</b>	Left > Right	1936	1925	1902	0.9976
	Right > Left	1858	1858	1830	0.9966
<b>HBN:</b>	Left > Right	695	691	685	0.9992

<b>Cerebellum</b>					
	<b>Right &gt; Left</b>	636	633	624	0.9985

899 **Table S6:** Replicating all HBN analyses in networks of interest: motor, somatosensory, language, as well as analyses  
900 in whole brain and cerebellum while controlling for clinical diagnoses. Table shows comparison between significant  
901 edges when controlling for clinical diagnoses, the overlapping edges between these two analyses and the correlation  
902 between the two analyses (reported as r values).